

◀ **Fig. 2** Changes from baseline in the regional wall thickness of the LV at 3 months and 1 year follow-up. **a–d** Images of the end-diastolic (**a, c**) and end-systolic (**b, d**) phase at baseline (**a, b**) and at the 3-month follow-up (**c, d**). The calculated wall thickness of each segment is shown in **e** (end-diastolic phase) and **f** (end-systolic phase), and the percent wall thickening is shown in **g**. The surgical specimens were obtained from the LV apical core removed at the time of LVAS implantation (**h**), and the needle biopsy of the LV anterior wall at the time of LVAS removal (**i**). Specimens were stained with hematoxylin–eosin (HE) by a conventional technique. **j** After LVAS implantation, the BNP level declined and reached a plateau. After myoblast sheet implantation, the BNP levels declined again to within the normal range

the anterior to lateral surface of the dilated heart through a left lateral thoracotomy.

Off-pump tests performed 8 weeks and 3 months after transplantation revealed that the ejection fraction was improved from 26 to 46%, and the LVDd from 49 to 53 mm (Fig. 1b, c). These data met the criteria for the explantation of LVAS, which was subsequently performed. Comparison of the wall motion pre- and post-treatment by color kinesis revealed improvement first on the anterior and lateral surfaces and then, in the longer term, on the other surface (Fig. 2). After starting the LVAS, the patient's brain natriuretic peptide (BNP) levels had gradually declined and reached a plateau. Subsequently, after myoblast sheet implantation, the BNP levels declined again and reached the normal range (Fig. 2j). The patient was discharged 7 months after myoblast sheet transplantation and has been an out-patient for more than 1 year. Regarding his clinical course after both cell sheet transplantation and LVAD removal, a Holter cardiogram demonstrated that no life-threatening arrhythmia had occurred.

Discussion

Menasche et al. [3] recently concluded that myoblast injections combined with coronary surgery in patients with depressed LV function fail to improve echocardiographic heart function. The proportion of injected cells surviving to engraft the infarcted myocardium is very low, owing to injected cells leaking from the intended region and being carried to other organs [4]. This loss of cells has therefore limited the applicability of this form of myoblast cell therapy [3].

To overcome these problems, we have developed a novel cell delivery system [5] that uses myoblast cell sheets, and performed animal investigations to guide clinical trials [4]. Using temperature-responsive tissue engineering techniques, we were able to transplant a larger numbers of cells, with

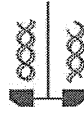
greater viability, than by myoblast injection, and such cell sheets engrafted to the failed myocardium in rats led to improvements in cardiac function and tissue remodeling [4]. Although the myoblasts cannot transdifferentiate to cardiomyocytes, the myoblast sheets produce cytokines such as hepatocyte growth factor (HGF), which may have a positive impact on c-Met-expressing damaged myocardium [4], thus leading to the attenuation of fibrosis, angiogenesis, and recruitment of stem cells induced by paracrine cytokines.

In cellular therapy for cardiac disease, arrhythmogenesis is expected to occur in animal models and in clinical trials [3]; however, life-threatening arrhythmias have not been clinically observed after autologous cell sheet transplantation. In the case of injection, scarring of the myocardium is likely, and such scars can induce arrhythmias. Using our cell delivery technique, there may be less risk for inducing arrhythmia. Myoblasts have a weak electrical potential, and it may thus be possible for them to induce arrhythmia if they survive in the myocardium. However, cell sheets may not induce arrhythmia owing to their attachment to the epicardium.

In conclusion, autologous myoblast cell sheet transplantation may positively contribute to the improvement of the clinical condition of patients with DCM, allow the discontinuation of LVAS, and avoid heart transplantation. This therapy therefore shows promise for clinical myocardial regeneration in patients with end-stage DCM.

References

1. Dandel M, Weng Y, Siniawski H, Potapov E, Lehmkuhl HB, Hetzer R. Long-term results in patients with idiopathic dilated cardiomyopathy after weaning from left ventricular assist devices. *Circulation*. 2005;112:137–45.
2. Hata H, Matsumiya G, Miyagawa S, et al. Grafted skeletal myoblast sheets attenuate myocardial remodeling in pacing-induced canine heart failure model. *J Thorac Cardiovasc Surg*. 2006;132:918–24.
3. Menasche P, Alfieri O, Janssens S, et al. The myoblast autologous grafting in ischemic cardiomyopathy (MAGIC) trial: first randomized placebo-controlled study of myoblast transplantation. *Circulation*. 2008;117:1189–200.
4. Memon IA, Sawa Y, Fukushima N, et al. Repair of impaired myocardium by means of implantation of engineered autologous myoblast sheets. *J Thorac Cardiovasc Surg*. 2005;130:1333–41.
5. Miyagawa S, Sawa Y, Sakakida S, et al. Tissue cardiomyoplasty using bioengineered contractile cardiomyocyte sheets to repair damaged myocardium: their integration with recipient myocardium. *Transplantation*. 2005;80:1586–95.



TECHNICAL NOTE

Evaluation of vertical cell fluidity in a multilayered sheet of skeletal myoblasts

Masahiro Kino-oka,^{1,*} Trung Xuan Ngo,² Eiji Nagamori,¹ Yasunori Takezawa,² Yasuki Miyake,² Yoshiki Sawa,³ Atsuhiko Saito,³ Tatsuya Shimizu,⁴ Teruo Okano,⁴ and Masahito Taya²

Department of Biotechnology, Graduate School of Engineering, Osaka University, 2-1 Yamada-oka, Suita, Osaka 565-0871, Japan,¹ Division of Chemical Engineering, Graduate School of Engineering Science, Osaka University, 1-3 Machikaneyama-cho, Toyonaka, Osaka 560-8531, Japan,² Department of Surgery, Division of Cardiovascular Surgery, Graduate School of Medicine, Osaka University, 2-15 Yamada-oka, Suita, Osaka 565-0871, Japan,³ and Institute of Advanced Biomedical Engineering and Science, Tokyo Women's Medical University, 8-1 Kawada-cho, Shinjuku-ku, Tokyo 162-8666, Japan⁴

Received 19 August 2011; accepted 5 September 2011
Available online 20 October 2011

The procedure for fabricating a multilayered cell sheet has been developed by combining multiple sheets using a thermo-responsive surface and stamp system. Confocal laser scanning microscopy revealed that the fluidity of a multilayered sheet of skeletal myoblasts could be estimated as vertical diffusivity and changed upon addition of dermal fibroblasts.

© 2011, The Society for Biotechnology, Japan. All rights reserved.

[**Key words:** Cell sheet; Skeletal myoblasts; Dermal fibroblasts; Cell migration; Sheet fluidity; Image processing]

Cell sheet engineering is emerging as an advanced technique for preparing scaffold-free 3-dimensional (3-D) tissue (1), not only for transplantation but also for *in vitro* research. A temperature-responsive poly-*N*-isopropylacrylamide (PIPAAm) grafted surface can be used to form a cell sheet without any enzymatic digestion, thereby which permits to retain an intact extracellular matrix (ECM) (1). Sasagawa et al. previously constructed a multilayered structure of skeletal muscle myoblast cells in which prevascular formation by endothelial migration was observed (2).

Cell migration in 3-D constructs plays an important role in physiological and pathological phenomena such as embryonic development, cell alignment, immune reaction, angiogenesis, and metastasis (3). Understanding the mechanisms of cell migration will be useful in the design of biomimetic structures and functional engineered tissues. Although the behaviors of cells on 2-D culture surfaces have been extensively investigated (4–7), spatial cell movement in 3-D tissues, especially with regard to vertical migration inside the tissue, has not been investigated due to the absence of methods to allow *in vitro* quantitative and reproducible measurements. In the present study, a five-layered skeletal myoblast sheet was fabricated as a 3-D model to evaluate vertical cell migration by confocal laser scanning microscopy and image processing.

Human skeletal muscle myoblasts (HSMs; Lot. No. 4F1618; Lonza Walkersville Inc., Walkersville, MD, USA) and human dermal fibroblasts (HDFs; Lot. No. 6F4296; Lonza Walkersville Inc.) were used in the experiments. According to procedures described elsewhere (5, 8), the subcultures of HSMs on laminin-coated surfaces were carried out at 37°C in an atmosphere of 5% CO₂ in Dulbecco's modified

Eagle's medium (DMEM; Sigma-Aldrich, St. Louis, MO, USA) containing 10% fetal bovine serum (FBS; Invitrogen, Grand Island, NY, USA) and antibiotics (100 U/cm³ penicillin G, 0.1 mg/cm³ streptomycin, and 0.25 mg/cm³ amphotericin B; Invitrogen).

As shown in Fig. 1A, starter cells harvested from the subcultures were stained using CellTracker Green™ and CellTracker Orange™ (Invitrogen) to exhibit fluorescently green and orange cells, respectively, according to commercially recommended protocol (5 μM for 15 min for live cell imaging). The stained cells were employed in the fabrication of the multilayered sheet according to newly developed procedures as follows. HSMs were seeded at 2.3 × 10⁵ cells/cm² in each well (diameter, 1.9 cm²) of 24-well UpCell™ plates (CellSeed, Tokyo) with a temperature-responsive surface grafted with PIPAAm and incubated for 24 h at 37°C in 5% CO₂ to form the monolayer sheet. The medium depth was set to 2 mm throughout the experiments and HDFs were mixed into the sheet if needed. For stacking monolayer cell sheets to form the multilayered cell sheet, a manipulator was designed as shown in Fig. 1B composed of a stamp, its stand, and a mold to load the stamp with the gelatin gel. A solution of 7.4% gelatin was prepared by dissolving gelatin powder (G1890-100G; Sigma-Aldrich) in 5 mL Hank's balance salt solution (Sigma-Aldrich) and 100 μL of 1 N NaOH solution at 45°C for 30 min. The solution was then sterilized by filtration through a 0.22-μm filter (Millex-GS; Millipore Co., Billerica, MA, USA) and poured into the silicone molds under aseptic conditions. The stamps were put onto the molds on ice to gelation. Finally, the molds were gently removed and the stamps with the gelatin were ready to be used to stack the cell sheets. To harvest the monolayer sheet, the stamp with the gelatin gel was overlaid on the monolayer sheet in a well at 37°C and the temperature was shifted to 20°C (Fig. 1A). After 30 min, the stamp was lifted together with the monolayer sheet from the bottom surface of the well. The steps were

* Corresponding author. Tel.: +81 6 6879 7444; fax: +81 6 6879 4246.
E-mail address: kino-oka@bio.eng.osaka-u.ac.jp (M. Kino-oka).

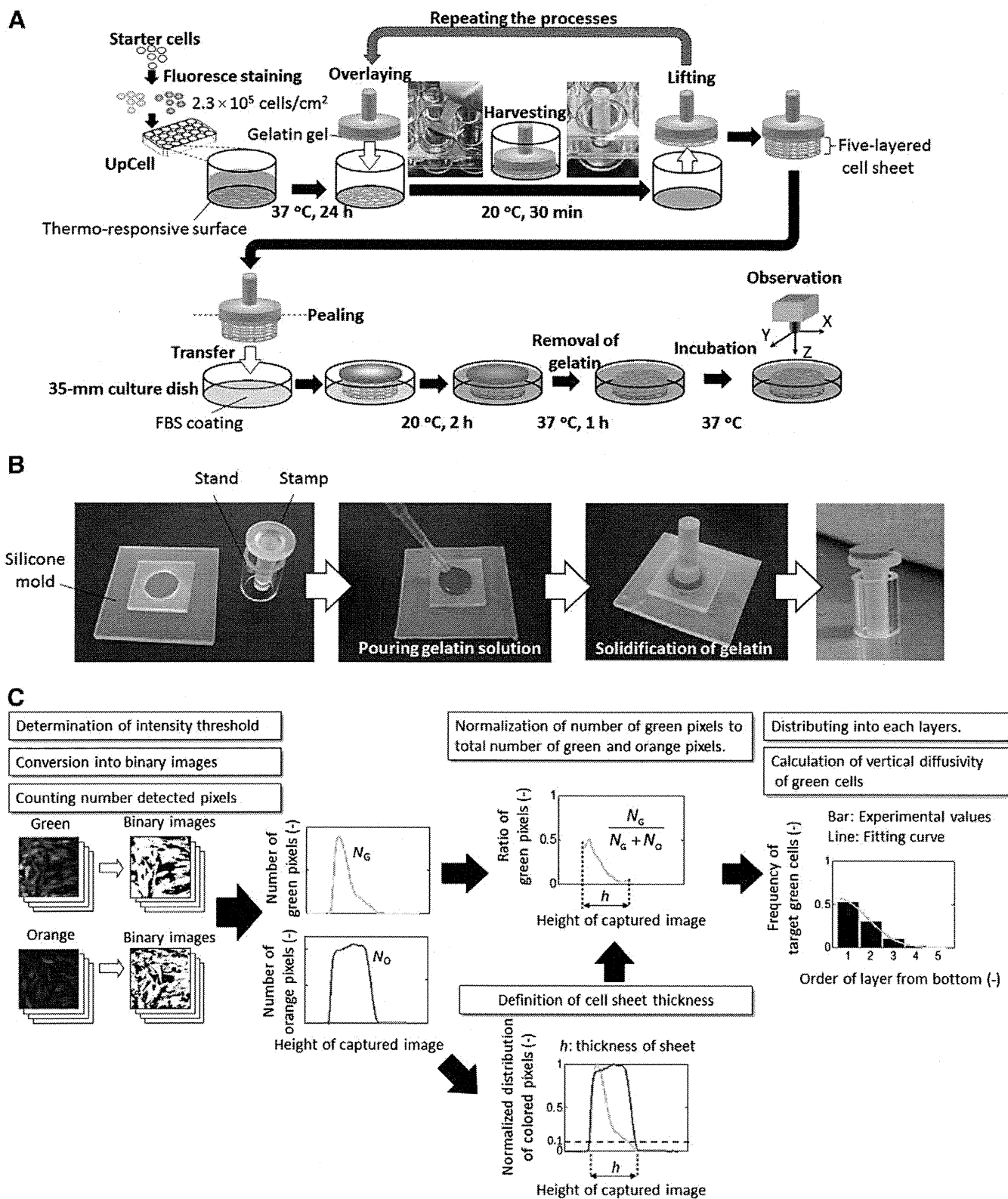


FIG. 1. Schematic diagrams showing the five-layered cell sheet fabrication and quantitative diffusivity analysis. (A) Fabrication of the five-layered cell sheet. (B) Preparation of the manipulator used to harvest the cell sheet. (C) Image processing system calculating the spatial distribution and diffusivity of the green target cells.

then repeated for the sequential harvests of monolayer sheets to form the multilayer structure on the stamp. The multilayered sheet with the gelatin was separated from the stamp and placed on a 35-mm culture dish (ibidi GmbH, Martinsried, Germany) that was precoated

with 0.2 mL/cm² FBS for 24 h for the facilitation of the sheet attachment to the surface, and the dish was incubated for 2 h at 20°C in 5% CO₂ without the addition of medium. To remove gelatin, the medium (0.4 mL/cm²) was added, and the temperature was

shifted to 37°C for 1 h to melt the gelatin and the medium was changed with a fresh one. In the present study, the fabricated culture system of a five-layered sheet was used to analyze sheet behaviors.

As a typical culture system, the five-layered sheet consisting of basal layers (green) and other layers (orange) stained by CellTracker Green™ and CellTracker Orange™, respectively, was prepared for the observation of tempo-spatial cell distribution using confocal laser scanning microscopes (FV10i for time lapse and FV-300 for spatial distribution; Olympus, Tokyo) with 60× objective lens. To determine the spatial distribution of the target cells, the green and orange cells in each layer at 0 and 48 h of incubation were observed and quantitatively analyzed using image processing (Fig. 1C). The five-layered sheet was washed twice with phosphate buffered saline (PBS) and then fixed with 4% paraformaldehyde in PBS (Wako Pure Chemical Industries, Osaka) overnight. After washing with PBS, at least eight random positions of each sample were scanned at a 0.6- μm interval to yield slice images for vertical direction determination. After intensity threshold values were identified, 8-bit images (256×256 pixels) of both colors in each slice were converted into binary images, leading to the distinction between colored and non colored pixels. Here the colored pixels which were derived from green and orange fluorescent original images denoted the green and orange pixels, respectively. The number of colored pixels in each slice was counted. The green and orange pixels in each slice were normalized using the maximum green and orange pixel values, respectively, found in all of the slice images. The slice possessing more than 10% of the colored pixels was regarded to exist inside cell sheet, from which the vertical positions at top and bottom of the five-layered sheet, and the sheet thickness, h , were determined. The ratio of green pixels to sum of green and orange pixels in each slice was normalized to determine the distribution of green pixels by dividing into 5 layers. Here, the normalized distribution of green pixels was assumed to be equivalent to the green cell distribution in the sheet, recorded by the frequency of green cells, f_G , in each layer.

Time-lapse observation was conducted of the five-layered sheet (Supplementary Movie S1). During the early incubation period, the green cells were observed in the bottom of the sheet, and the active cellular migration occurred in the horizontal and vertical directions anywhere in the sheet, revealing the sheet fluidity. The green cells then migrated toward the upper layers as time elapsed. To understand the extent of the sheet fluidity, the vertical distribution of green cells was estimated. Figure 2 shows the histograms of f_G at 0 and 48 h. The f_G values in the first and second layers from the bottom surface were estimated to be $f_G = 0.82$ and 0.17, respectively, and the sheet at 48 h had a broad distribution of f_G , being $f_G = 0.37$ in the first layer. In addition, the f_G decreased gradually along the layers from bottom to top, suggesting the analogy of vertical migration to molecular diffusion. To quantitatively analyze vertical sheet fluidity, the diffusivity, D , was determined based on Fick's second law, $\frac{\partial f_G}{\partial t} = D \frac{\partial^2 f_G}{\partial h^2}$, in which f_G , t , and h represent the green cell frequency, incubation time, and sheet thickness,

respectively. The Crank-Nicolson finite difference method and least squares method were applied to calculate the diffusivity using a custom-made software programmed by LabVIEW (National Instruments, Austin, TX, USA). The initial condition was that the total ratio of green cells in the five layers was normalized to unity. The free boundary condition, $\frac{df_G}{dh} = 0$, is set at both the bottom and the top of the five-layered sheet. In a practical aspect, the f_G distribution data at 0 and 48 h were applied to calculate the apparent vertical diffusivity of green cells, \bar{D}_o , being $\bar{D}_o = 0.74 \mu\text{m}^2/\text{h}$ (Table 1).

To investigate sheet fluidity variation, we incubated five-layered sheets added with HDFs comprising 25% and 50% of the cell counts (conditions B and C, respectively). As shown in Table 1, the \bar{D}_o increased at 25% addition (condition B) compared to that without any HDF addition (condition A), although the significance level was not sufficient ($p < 0.06$). In addition, 50% addition (condition C) caused a decrease in \bar{D}_o compared to that at 25% addition ($p < 0.05$). For further understanding of the role of HDFs addition, we established the five-layered sheet system composed of HSMs or HDFs in basal layer stained by CellTracker Green™ and the rest of cells stained by CellTracker Orange™, and estimated the diffusivity of basal HSMs or HDFs, \bar{D}_M or \bar{D}_F , respectively (Table 1). At 25% addition, \bar{D}_F was estimated to be $2.40 \mu\text{m}^2/\text{h}$, being 4 times larger than \bar{D}_M . At 50% addition, \bar{D}_F decreased to $0.80 \mu\text{m}^2/\text{h}$, although \bar{D}_M stayed constant, suggesting that \bar{D}_o depended on HDF migration in the sheet.

An independent experiment showed that the migration rate of single HDF is 1.5 times higher than that of single HSMs in culture using a conventional T-flask (data not shown). Pittet et al. reported that HDFs exhibited strong OB-cadherin connection in high-density culture (9). These results suggest that HDF active migration physically facilitated the overall fluidity in the sheet at lower HDF addition levels. It is most likely that higher HDF addition induced strong HDF intracellular binding in the sheet, and this strong interaction with lower HDF migration rates resulted in the decline of overall sheet fluidity.

The inner structural fluidity of cells in 3-D constructs has been reported in cultured neurospheres (10) and embryoid bodies (11). In static suspension cultures of mouse neural stem cells, active migration of single cells caused aggregate formation through intercellular coalescence, and culture prolongation led to cell division in the aggregates as well as accidental coalescence between independent aggregates that formed large spheres in which the location of distribution of differentiated neurons and glia was observed (12). Further observation revealed that the large sphere was caused by spontaneous active migration in aggregates through the live-cell imaging technique. In addition, Duguay et al. (13) reported that aggregation using a mixture of E-cad-expressing E8a cell line and P-cad-expressing LP1 cell line caused spatial habitat isolation of 3-D spheres via active cell migration and intercellular binding affinity, leading to autonomous double-layer spheres by different cell types. These results mean the importance of cell migration in 3-D constructs

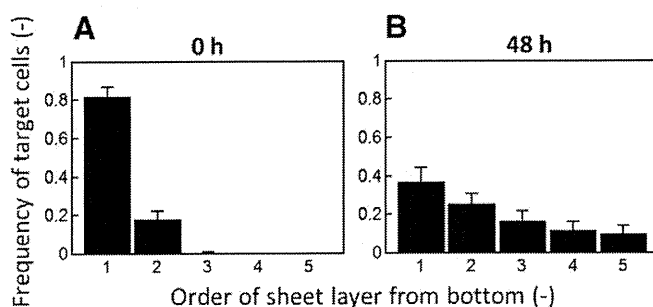


FIG. 2. Spatial distributions of the green target cells inside the cell sheet at 0 (A) and 48 h (B). Bars show the standard deviation (SD) ($n = 3$).

TABLE 1. Diffusivities of different target cells from the basal layer in the five-layered cell sheet at different cellular balance conditions.

Condition	HSMs (%)	HDFs (%)	Initial thickness of sheet, h (μm)	Diffusivity ($\mu\text{m}^2/\text{h}$)		
				\bar{D}_o	\bar{D}_M	\bar{D}_F
A	100	0	33.0 ± 5.4	0.74 ± 0.23	–	–
B	75	25	36.4 ± 5.4	1.57 ± 0.50	0.57 ± 0.14	2.40 ± 0.49
C	50	50	37.7 ± 5.0	0.69 ± 0.12	0.54 ± 0.26	0.80 ± 0.36

\bar{D}_o , \bar{D}_M , and \bar{D}_F are the diffusivities of whole cells, skeletal myoblasts, and dermal fibroblasts from the basal layer, respectively. HSMs, human skeletal muscle myoblasts; HDFs, human dermal fibroblasts. All values were expressed as mean \pm SD ($n = 3$).

affecting the fate of stem cells as well as spatial habitat isolation of differentiated cells. In the current study, HDF addition was found to affect sheet fluidity. Further experiments clarified the localization of HDFs in five-layered sheets (Oda, M. et al., Abstr., 10th Congress of the Japanese Society for Regenerative Medicine, p. 248, 2011). This finding suggested that the cell sheet fabricated from HMMs and HDFs exhibited the habitat isolation between them.

Many researchers have paid much attention to tissue mimicry by using cellular aggregates, which are considered minimized functional structures. The mimic constructs have broad potential use as transplants in regenerative medicine as well as structural material for elucidating the dynamic tissue development mechanism. From the standpoint of analytical techniques, observational convenience of 3-D constructs is a critical requirement because cellular behaviors such as migration, division, and communication affect the common mechanisms of tissue development.

In conventional studies, most of the techniques for fabricating cell aggregates led to spherically shaped constructs through spontaneous formation by cellular coagulation. In contrast, the current system applied the plate shape of the multilayered sheet using artificially designed formation by the assembly of monolayer sheets because the mimic system using the plate-shaped aggregate has the observational advantage in the 3-D construct. The plate-shaped aggregates can be fabricated in various ways using cell sheet engineering technique with thermo-responsive polymer grafted surface (1), biodegradable peptide grafted surface (14) or collagenase degradable atelocollagen film (15), magnetic-force based tissue engineering technique (16), layer-by-layer assembly technique with ECM coating cells (17), compressed collagen sheet (18), vitrified collagen film "vitrigel" (19), and bioprinting method (20).

Our system that uses multilayered sheet containing stained target cells in the basal layer and confocal laser scanning microscopy realizes clear observation of target cell behaviors in the vertical direction, enabling monodimensional analysis of vertical cell distribution inside the sheet. The reduced spatial dimension makes easy to analyze cell migration, compared to the full 3-D analysis required of spherically shaped aggregates. Thus, the system developed in the present study can be a powerful tool for elucidating dynamic phenomena in 3-D constructs.

Supplementary data to this article can be found online at doi:10.1016/j.jbiosc.2011.09.001.

This study was supported by the New Energy and Industrial Technology Development Organization (NEDO) of Japan, and the Japan Society for the Promotion of Science (JSPS) through the "Funding Program for World-Leading Innovative R&D on Science and Technology (FIRST Program)," initiated by the Council for Science and Technology Policy (CSTP).

References

1. Yang, J., Yamato, M., Kohno, C., Nishimoto, A., Sekine, H., Fukai, F., and Okano, T.: Cell sheet engineering: recreating tissues without biodegradable scaffolds, *Biomaterials*, **26**, 6415–6422 (2005).
2. Sasagawa, T., Shimizu, T., Sekiya, S., Haraguchi, Y., Yamato, M., Sawa, Y., and Okano, T.: Design of prevascularized three-dimensional cell-dense tissues using a cell sheet stacking manipulation technology, *Biomaterials*, **31**, 1646–1654 (2010).
3. Horwitz, R. and Webb, D.: Cell migration, *Curr. Biol.*, **13**, R756–R759 (2003).
4. Louis, M., Zanou, N., Van, S. M., and Gailly, P.: TRPC1 regulates skeletal myoblast migration and differentiation, *J. Cell Sci.*, **121**, 3951–3959 (2008).
5. Chowdhury, S. R., Muneyuki, Y., Takezawa, Y., Kino-oka, M., Saito, A., Sawa, Y., and Taya, M.: Synergic stimulation of laminin and epidermal growth factor facilitates the myoblast growth through promoting migration, *J. Biosci. Bioeng.*, **108**, 174–177 (2009).
6. Wang, W., Pan, H. Y., Murray, K., Jefferson, B. S., and Li, Y.: Matrix metalloproteinase-1 promotes muscle cell migration and differentiation, *Am. J. Pathol.*, **174**, 541–549 (2009).
7. Bondesen, B. A., Jones, K. A., Glasgow, W. C., and Pavlath, G. K.: Inhibition of myoblast migration by prostacyclin is associated with enhanced cell fusion, *FASEB J.*, **21**, 3338–3345 (2007).
8. Chowdhury, S. R., Muneyuki, Y., Takezawa, Y., Kino-oka, M., Saito, A., Sawa, Y., and Taya, M.: Growth and differentiation potentials in confluent state of culture of human skeletal muscle myoblasts, *J. Biosci. Bioeng.*, **109**, 310–313 (2010).
9. Pittet, P., Lee, K. M., Kulik, A. J., Meister, J. J., and Hinz, B.: Fibrogenic fibroblasts increase intercellular adhesion strength by reinforcing individual OB-cadherin bonds, *J. Cell Sci.*, **121**, 877–886 (2008).
10. Singec, I., Knoth, R., Meyer, R. P., Maciarczyk, J., Volk, B., Nikkhah, G., Frotscher, M., and Snyder, E. Y.: Defining the actual sensitivity and specificity of the neurosphere assay in stem cell biology, *Nat. Methods*, **3**, 801–806 (2006).
11. Dang, S. M., Kyba, M., Perlingeiro, R., Daley, G. Q., and Zandstra, P. W.: Efficiency of embryoid body formation and hematopoietic development from embryonic stem cells in different culture systems, *Biotechnol. Bioeng.*, **78**, 442–453 (2002).
12. Mori, H., Ninomiya, K., Kanemura, Y., Yamasaki, M., Kino-oka, M., and Taya, M.: Image cytometry for analyzing regional distribution of cells inside human neurospheres, *J. Biosci. Bioeng.*, **103**, 384–387 (2007).
13. Duguay, D., Foty, R. A., and Steinberg, M. S.: Cadherin-mediated cell adhesion and tissue segregation: qualitative and quantitative determinants, *Dev. Biol.*, **253**, 309–323 (2003).
14. Qiu, F., Chen, Y., Cheng, J., Wang, C., Xu, H., and Zhao, X.: A simple method for cell sheet fabrication using mica surfaces grafted with peptide detergent A(6)K, *Macromol. Biosci.*, **10**, 881–886 (2010).
15. Nagai, N., Yunoki, S., Satoh, Y., Tajima, K., and Munekata, M.: A method of cell-sheet preparation using collagenase digestion of salmon atelocollagen fibrillar gel, *J. Biosci. Bioeng.*, **98**, 493–496 (2004).
16. Ito, A., Shinkai, M., Honda, H., and Kobayashi, T.: Medical application of functionalized magnetic nanoparticles, *J. Biosci. Bioeng.*, **100**, 1–11 (2005).
17. Matsusaki, M., Kadowaki, K., Nakahara, Y., and Akashi, M.: Fabrication of cellular multilayers with nanometer-sized extracellular matrix films, *Angew. Chem. Int. Ed.*, **46**, 4689–4692 (2007).
18. Brown, R. A., Wiseman, M., Chuo, C. B., Cheema, U., and Nazhat, S. N.: Ultrarapid engineering of biomimetic materials and tissues: fabrication of nano- and microstructures by plastic compression, *Adv. Funct. Mater.*, **15**, 1762–1770 (2005).
19. Takezawa, T., Ozaki, K., Nitani, A., Takabayashi, C., and Shimo-Oka, T.: Collagen vitrigel: a novel scaffold that can facilitate a three-dimensional culture for reconstructing organoids, *Cell Transplant.*, **13**, 463–473 (2004).
20. Nakamura, M., Iwanaga, S., Henmi, C., Arai, K., and Nishiyama, Y.: Biomaterials and biomaterials for future developments of bioprinting and biofabrication, *Biofabrication*, **2**, 014110 (2010).

Role of Epithelial-Stem Cell Interactions during Dental Cell Differentiation^{*S}

Received for publication, August 4, 2011, and in revised form, January 5, 2012. Published, JBC Papers in Press, February 1, 2012, DOI 10.1074/jbc.M111.285874

Makiko Arakaki^{‡1}, Masaki Ishikawa^{S1}, Takashi Nakamura[‡], Tsutomu Iwamoto[‡], Aya Yamada[‡], Emiko Fukumoto[‡], Masahiro Saito[¶], Keishi Otsu^{||}, Hidemitsu Harada^{||}, Yoshihiko Yamada^S, and Satoshi Fukumoto^{‡2}

From the [‡]Division of Pediatric Dentistry, Department of Oral Health and Development Sciences, Tohoku University Graduate School of Dentistry, Sendai 980-8575, Japan, the ^SLaboratory of Cell and Developmental Biology, NIDCR, National Institutes of Health, Bethesda, Maryland 20892, the [¶]Faculty of Industrial Science and Technology, Tokyo University of Science, Chiba 278-8510, Japan, and the ^{||}Department of Oral Anatomy II, Iwate Medical College School of Dentistry, Morioka 020-8505, Japan

Background: The role of dental epithelium in stem cell differentiation has not been clearly elucidated.

Results: SP cells differentiated into odontoblasts by epithelial BMP4, whereas iPS cells differentiated into ameloblasts when cultured with dental epithelium.

Conclusion: Stem cells can be induced to odontogenic cell fates when co-cultured with dental epithelium.

Significance: This is the first report to show induction of ameloblasts from iPS cells.

Epithelial-mesenchymal interactions regulate the growth and morphogenesis of ectodermal organs such as teeth. Dental pulp stem cells (DPSCs) are a part of dental mesenchyme, derived from the cranial neural crest, and differentiate into dentin-forming odontoblasts. However, the interactions between DPSCs and epithelium have not been clearly elucidated. In this study, we established a mouse dental pulp stem cell line (SP) comprised of enriched side population cells that displayed a multipotent capacity to differentiate into odontogenic, osteogenic, adipogenic, and neurogenic cells. We also analyzed the interactions between SP cells and cells from the rat dental epithelial SF2 line. When cultured with SF2 cells, SP cells differentiated into odontoblasts that expressed dentin sialophosphoprotein. This differentiation was regulated by BMP2 and BMP4, and inhibited by the BMP antagonist Noggin. We also found that mouse iPS cells cultured with mitomycin C-treated SF2-24 cells displayed an epithelial cell-like morphology. Those cells expressed the epithelial cell markers p63 and cytokeratin-14, and the ameloblast markers ameloblastin and enamelin, whereas they did not express the endodermal cell marker Gata6 or mesodermal cell marker brachyury. This is the first report of differentiation of iPS cells into ameloblasts via interactions with dental epithelium. Co-culturing with dental epithelial cells appears to induce stem cell differentiation that favors an odontogenic cell fate, which may be a useful approach for tooth bioengineering strategies.

Tooth morphogenesis is characterized by reciprocal interactions between dental epithelium and mesenchymal cells derived from the cranial neural crest, which result in formation of the proper number and shapes of teeth. Multiple extracellular signaling molecules, including BMPs, FGFs, WNTs, and SHH, have been implicated in these interactions for tooth development (1). Epithelial cells then subsequently give rise to enamel-forming ameloblasts, while mesenchymal stem cells (MSCs)³ form dentin-forming odontoblasts and dental pulp cells. Initial tooth development is also regulated by extracellular matrices (ECMs), such as basement membrane components that include laminin, collagen, fibronectin, and perlecan (2, 3). These matrices control proliferation, polarity, and attachment, and also determine tooth germ size and morphology. At later stages of tooth development, the basement membrane components disappear and odontogenic cells begin to secrete a variety of tooth-specific extracellular matrices that give rise to layers of enamel and dentin, produced by epithelial-derived ameloblasts and mesenchymal-derived odontoblasts, respectively. Ameloblastin (Ambn) is one of the enamel matrix proteins expressed by differentiating ameloblasts, and is essential for dental epithelial cell differentiation into ameloblasts and enamel formation (2, 4). Dentin sialophosphoprotein (DSPP) is a member of the SIBLING (Small Integrin-Binding Ligand N-linked Glycoprotein) family of extracellular matrix glycoprophosphoproteins, and is expressed by differentiating ameloblasts and odontoblasts (5). These extracellular matrices are important for the formation of enamel and dentin (2).

Stem cell research has identified and established several types of stem cells, including induced pluripotent stem (iPS) cells, which are generated from a variety of somatic cell types via introduction of transcription factors that mediate pluripo-

* This work was supported, in whole or in part, by the Intramural Research Program of the NIDCR, National Institutes of Health (to Y. Y.). This work was also supported by Grants-in-aid 20679006 (to S. F.), 21792054 (to A. Y.), 21792154 (to E. F.) from the Ministry of Education, Science, and Culture of Japan, and the NEXT program (LS010, to S. F.), and by grants from the Takeda Science Foundation.

^S This article contains supplemental Figs. S1–S5 and Table S1.

¹ Both authors contributed equally to this work.

² To whom correspondence should be addressed: Division of Pediatric Dentistry, Department of Oral Health and Development Sciences, Tohoku University Graduate School of Dentistry, Sendai 980-8575, Japan. Fax: 81-22-717-8386; E-mail: fukumoto@dent.tohoku.ac.jp.

³ The abbreviations used are: MSC, mesenchymal stem cell; mDP, mouse dental pulp; Ambn, Ameloblastin; DSPP, dentin sialophosphoprotein; iPS, induced pluripotent stem; DPSC, dental pulp stem cell; SP, side population; MP, majority population; ALP, alkaline phosphatase; MEF, mouse embryonic fibroblasts; MMC, mitomycin C.

tency (6). Direct reprogramming of somatic cells into iPS cells by forced expression of a small number of defined factors (e.g. Oct3/4, Sox2, Klf4, and c-Myc) has great potential for tissue-specific regenerative therapies. In addition, this process also avoids ethical issues surrounding the use of embryonic stem (ES) cells, as well as problems with rejection following implantation of non-autologous cells (7). A variety of cell types, including hematopoietic precursor cells (8, 9), endothelial cells, MSCs, neuronal cells (10), reproductive cells (11), and cardiomyocytes (12, 13), undergo *in vitro* differentiation. However previous studies of dental cell differentiation are not adequate to explain this process. Several dental stem cell populations have been identified in different parts of the tooth, including cells from the periodontal ligament that links the tooth root with the bone, tips of developing roots, and tissue (dental follicle) that surrounds an unerupted tooth. In addition, dental pulp stem cells (DPSCs) have been identified in the pulp of exfoliated deciduous teeth of both children and adults (14). These different cell types likely share a common lineage, being derived from neural crest cells, and all have generic MSC-like properties.

Transplantation of *in vitro* expanded DPSCs mixed with hydroxyapatite/tricalcium phosphate particles results in the formation of dental pulp and dentin-like tissue complexes in immunocompromised mice (15). Similar results have been observed with an MSC population obtained from human exfoliated deciduous teeth (SHED) (14). DPSCs also express the putative stem cell marker STRO-1 and perivascular cell marker CD146, while a proportion co-expresses smooth muscle actin and the pericyte-associated antigen 3G5 (16). These findings suggest that a population of DPSCs may reside in this perivascular niche within the pulp of adult teeth.

Side population (SP) cells were identified by flow cytometry analysis with a Hoechst 33342 efflux assay and found to have stem cell characteristics (17). SP cells are a small population that show low levels of Hoechst dye staining for the expression of Abcg2, an ATP-binding cassette transporter (18), which is strongly expressed in dental pulp in human adult and deciduous teeth (19). Dental pulp contains multipotent stem cells and is viewed as a potential source of iPS cells (14, 20, 21). In tooth germ development, undifferentiated neural crest-derived MSCs interact with dental epithelium and differentiate into dentin matrix-secreting odontoblasts. However, the interactions between stem cells and dental epithelium have not been clearly elucidated.

In this study, we established an SP cell line from mouse dental papilla. We then cultured these SP cells with rat dental epithelial cells to investigate epithelial-mesenchymal interactions. SP cells were induced to differentiate into DSPP expressing odontoblasts via the action of epithelial BMP4. Furthermore, mouse iPS cells differentiated into Ambn-expressing dental epithelium when cultured with dental epithelial cells. Thus, these undifferentiated stem cells can be induced to an odontogenic cell fate when co-cultured with dental epithelial cells. These findings may be useful for analysis of dental cell differentiation *in vitro* and for procurement of odontogenic cells for use in regenerative medicine.

EXPERIMENTAL PROCEDURES

Preparation of Mouse Dental Papilla Cells—Dental papilla tissues were isolated from incisors from newborn ICR mice by digesting with 0.1% collagenase D (Roche) and 2.5% trypsin for 30 min at 37 °C. Enzymatically digested tissues were minced into 2–4 mm pieces using micro-scissors and washed three times with Dulbecco's modified Eagle's medium (DMEM) (Invitrogen) containing 10% fetal bovine serum (FBS) (Invitrogen) and an antibiotic-antimycotic mixture (Invitrogen), then filtered through a cell strainer (40 μ m) to eliminate clumps and debris. Mouse dental papilla (mDP) cells were cultured in 60-mm culture dishes and immortalized by expression of a mutant human papilloma virus type 16 E6 gene lacking the PDZ-domain-binding motif (22). mDP cells were maintained with DMEM supplemented with 10% FBS and an antibiotic-antimycotic mixture at 37 °C in a humidified atmosphere containing 5% CO₂.

Generation of Dental Epithelial Cell Line SF2-24 and Cell Culture—Rat dental epithelial cells were enzymatically isolated from the cervical loop at the apical end of the lower incisors from a Sprague-Dawley rat with 1% collagenase. Dental epithelial cells were cultured with DMEM (Invitrogen) supplemented with 10% FBS for 4 weeks, then, maintained in serum-free keratinocyte synthetic medium (Keratinocyte-SFM, Invitrogen) for 1 year. An established cell line, SF2 was maintained as previously described (4). SF2 cells were transfected with a pEF6/GFP-PDGFm-myc-HA vector expressing the GFP-PDGF receptor-transmembrane fusion protein with myc-HA tag using Lipofectamine 2000 (Invitrogen). Transfected cells were selected as SF2 subclones by culturing with media containing 400 μ g/ml of G418. Twenty-five clones were selected as a stable transfected cell line, with one of them designated as SF2-24 (Ambn high expression) and another SF2-7 (Ambn low expression).

SP and MP Cell Analysis and Flow Cytometry—Hoechst staining of mDP cells for SP cell analysis was conducted as previously described (17). Subconfluent mDP cells were stained with Hoechst dye for 90 min at 37 °C. After staining, all cells were resuspended in 100 μ l of Hanks' balanced salt solution (HBSS) with calcium/magnesium medium and kept on ice. The SP and MP gates were defined as previously described (17). For analysis, the cells were resuspended in ice-cold HBSS with 2% FBS containing propidium iodide (Sigma) at a final concentration of 2 μ g/ml to identify dead cells, then filtered through a cell strainer. Sorting and analyses were carried out with an EPICS ALTRA flow cytometer (Beckman Coulter, Fullerton, CA). The SP cell fraction was enriched by repeating cell sorting 3 times. The expression of stem cell markers in SP cells was confirmed by flow cytometry using anti-Sca-1 and Oct3/4 antibodies (Santa Cruz Biotechnology).

Differentiation of SP Cells—For odontoblastic induction, SP cells were plated at 6×10^4 cells in 60-mm dishes. After the cells had reached 50–60% confluence, we replaced the control medium with induction medium containing 100 ng/ml of BMP2 or BMP4 (Wako Pure Chemical Industries), and cells were incubated for 2 days. For blocking BMP signaling, recombinant mouse Noggin protein (R&D systems) was

Epithelial-Stem Cell Interactions during Dental Cell Differentiation

used. Total RNA was isolated and real time RT-PCR was performed using mouse Bcrp1 (18) and DSPP primer sets (supplemental Table S1).

For adipogenic differentiation, SP cells were seeded at 1×10^5 cells per well in 6-well plates and cultured in DMEM supplemented with 10% FBS. Adipogenic differentiation was induced with induction medium from a Poietics hMSC Media Bullet kit (Cambrex Bio Science Walkersville, Inc., Walkersville, MD) for 3 days and incubated in maintenance medium for 3 days, then the cells were cultured for an additional 7 days in maintenance medium. As a control, cells were cultured in only maintenance medium. Adipogenesis was confirmed by staining with Oil-Red-O and the expression of *PPAR* γ was analyzed by RT-PCR.

For osteogenic differentiation, SP cells were seeded at 1.5×10^4 cells per well in 6-well plates and cultured in DMEM supplemented with 10% FBS, 10 mM β -glycerophosphate, 0.2 mM ascorbic acid, 2-phosphate, and 10^{-8} M dexamethasone. Induction and control media were replaced every 2 days. Osteogenesis was determined by alkaline phosphatase (ALP) and von Kossa staining for calcium deposition, as previously described (23). After 4 weeks culturing with osteoblast induction medium, the expressions of osteocalcin, osteonectin, and Runx2 in osteogenesis-induced SP cells were analyzed by RT-PCR.

For neurogenic differentiation, we modified a neuronal induction protocol using recombinant nerve growth factor (NGF) (Chemicon). SP cells were seeded at 1×10^5 cells per well in 6-well plates. After reaching 80–90% confluence, neurogenic differentiation was induced by culturing the cells in DMEM supplemented 2% FBS, 1.25% dimethyl sulfoxide, 10^{-6} M retinoic acid, 2.5 μ g/ml insulin, and 50 ng/ml NGF. Two weeks later, neurogenesis was characterized by Western blot analysis using an anti-neurofilament-M specific antibody (Cell Signaling Technology).

Odontoblastic Induction of SP Cells by Co-culturing with Dental Epithelial Cells—We investigated the role of dental epithelial cells in specification of odontogenic cell lineage using two types of co-culture systems: feeder and chamber types with a cell culture insert (BD Falcon). We used confluent SF2 cells, or SF2 cells treated with 4% paraformaldehyde (PFA) or ammonium (denudation) as feeder cells. SF2 and SP cells were harvested and placed into either 6-well plates or cell culture inserts (chamber), then cultured until reaching confluence.

Screening of Co-culture Conditions for Ameloblastic Induction of iPS Cells—A mouse iPS cell line (iPS-MEF-Ng-20D-17), carrying the Nanog-GFP/IRES/puromycin resistant gene, was established by Yamanaka (Kyoto University, Japan), and obtained from RIKEN Cell Bank (Saitama, Japan) (6). Mouse iPS cells were cultured with rat dental epithelial cells (SF2-24), which predominantly express *Ambn* mRNA, as feeder cells. Preparatory co-culture experiments were performed as follows: iPS cells were cultured with mouse embryonic fibroblasts (MEFs) treated with mitomycin C (MMC) or with three different types of SF2-24 feeder cells (confluent cells, cells treated with MMC, cells treated with 4% PFA). MMC was supplied at 9 μ g/ml (final concentration) for 2 h to arrest SF2-24 cell proliferation.

Induction of iPS Cell-derived Ameloblasts—iPS cells (plated 1.5×10^3 /cm²) were cultured on sheets of MMC-treated SF2-24 cells for 7, 10, and 14 days in the same medium used for the SF2-24 culture without leukemia inhibitory factor and 2-mercaptoethanol. The culture medium was changed every day throughout the co-culture period. After 7 and 10 days, the co-cultured iPS cells were subjected to RT-PCR, while those after 14 days of culture were analyzed by immunocytochemistry. Total RNA from iPS cells co-cultured with MMC-treated MEFs was isolated after 3 days of culture. Conditioned media from cultures of SF2-24 and SF2-7 were collected after 2 days of incubation. The procedures used for transfection of *Ambn*-expressing vectors, as well as their construction and isolation of recombinant proteins have been previously described (2, 24). K252a (Trk inhibitor, Calbiochem), PD98059 (MEK inhibitor, Cell signaling), anti-NT-4 neutralizing antibody (Applied Biological Materials), and Noggin (R&D systems) were added to conditioned medium obtained from SF2-24 cells.

Reverse Transcription-PCR—Total RNA was isolated using TRIzol (Invitrogen) and first-strand cDNA was synthesized at 50 °C for 50 min using oligo(dT) or random primers with the SuperScript III First-strand Synthesis System (Invitrogen). PCR was performed with Takara Ex Taq HotStart Version (Takara) or a PCR Additives Kit (Jena Bioscience, Germany). The primer sequences are presented in supplemental Table S1. PCR amplicons were separated and visualized on 1.5% agarose gels with SYBR Green staining using the LAS-4000 mini image analyzing system (Fujifilm). For semi-quantitative PCR analysis, the band intensities of PCR amplicons were quantified using MultiGauge software (Fujifilm) and normalized by dividing the intensity of the band of GAPDH. Because of the high degree of homology between the *Ambn* gene in mice and rats (94.2%), we designed a species-specific mouse *Ambn* primer that encoded locked nucleic acid (LNA) at a different base sequence between the mouse and rat *Ambn* gene in a conserved region. The specificity of the mouse *Ambn* primer was confirmed by PCR using mouse and rat tooth germ cDNA. Statistical analysis of gene expression was performed using the Student's *t* test.

Immunocytochemistry—For immunocytochemistry, cells were fixed with 4% PFA for 5 min at room temperature. After washing with PBS three times for 5 min, the cells were treated with Power Block Universal Reagent (BioGenex) for 5 min at room temperature, followed by three washes with PBS. The cells were incubated with the anti-*Ambn* primary antibody included in the kit (1:200, M-300, Santa Cruz Biotechnology). The primary antibody was visualized with Alexa Fluor 594 donkey anti-rabbit antibody (1:500, A21207, Invitrogen). Nuclei were stained with Hoechst 33258 (Invitrogen). Immunocytochemistry and phase images were captured using a BZ-8000 microscopic system (KEYENCE Co, Osaka, Japan), and images of the sections were analyzed using a BZ analyzer (KEYENCE).

RESULTS

Establishment of SP Cell Line from Mouse Dental Papilla Cells—Side population (SP) cells, which displayed stem cell ability, make up less than 1% of total cells in the mouse dental papilla (mDP) from postnatal tooth germs. Thus, biochemical and biomolecular analyses of SP cells are difficult to perform

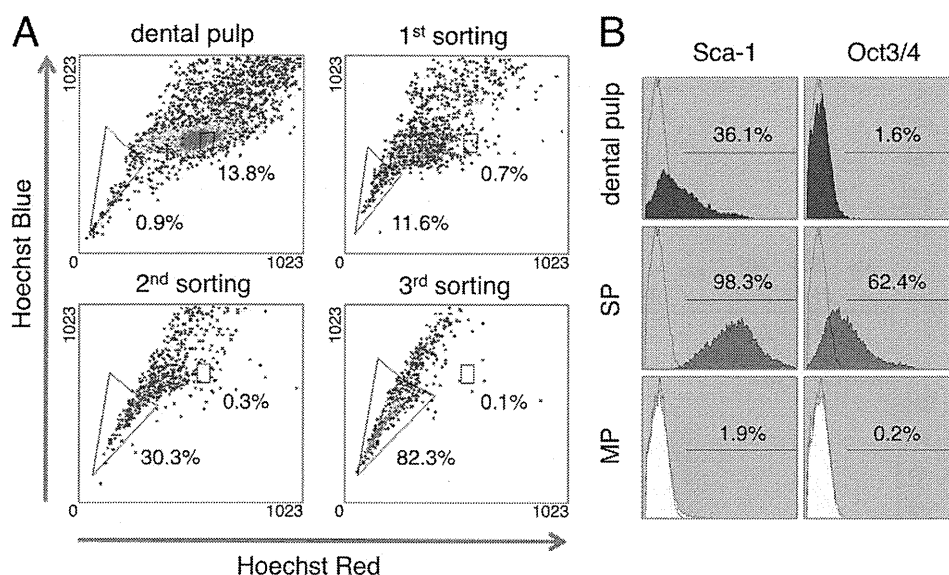


FIGURE 1. **Isolation of SP cells from mDP cell line.** A, flow cytometry analysis of SP cells. mDP cells made up ~0.9% of the total cell population with a relatively lower level of Hoechst 33342 fluorescence (SP cells), while 13.8% of the population was maintained as MP cells. Using repeated cell sorting, the SP cell population was enriched by 11.6% at the first sorting, 30.3% at the second sorting, and 82.3% at the third sorting. B, expression of the stem cell markers Sca-1 and Oct3/4 in dental pulp, SP, and MP cells.

because of the limited numbers of cells available. We enriched an SP cell population and established an SP cell line using a cell sorting technique. mDP cells were obtained from mouse incisor tooth germs and immortalized, as previously described (22). The cells were then stained with Hoechst dye and sorted to enrich the SP cell fraction. Cell sorting was repeated three times and SP cells were enriched from about 0.9% to 82.3% in the gated area (Fig. 1A). This SP cell line showed high expression levels of the stem cell markers Sca-1 and Oct3/4 when compared with the majority population (MP) cells, which was comprised of a greater number dental papilla cells in various differentiation stages (Fig. 1B).

Because the SP cells expressed a set of stem cell markers, we examined their multipotency. Using an odontoblast differentiation medium containing BMP2 or BMP4, the SP cells were induced to express DSPP, a marker of odontoblasts, whereas the expression of the undifferentiated cell marker Bcrp1 was decreased (Fig. 2A). In osteoblast differentiation medium, the SP cells showed increased levels of ALP and von Kossa staining, as well as expressions of the osteoblast marker genes osteocalcin, osteonectin, and Runx2, whereas the MP cells showed no induction of expression of those genes (Fig. 2, B and C). When SP cells were cultured in differentiation medium for adipogenesis or neurogenesis, they were Oil-Red-O positive or showed neurite outgrowths, along with high levels of adipogenic expression and protein expressions of neurogenic markers, such as PPAR γ and Neurofilament-M, respectively (supplemental Fig. S1, A--D). These results suggest that the SP cell line established in this study has a high level of multipotency.

Expressions of Runx2 and DSPP in SP Cells Cultured with SF2 Cells—We analyzed epithelial and mesenchymal stem cell interactions by culturing SP cells with rat dental epithelial SF2 cells that had been engineered to express a GFP-myc-HA tag on the cell membrane surface. This allowed us to distinguish between SP and SF2 cell types (supplemental Fig. S2). SP cells

were cultured with or without SF2 cells for 48 h, and total RNA was isolated from the mixed cell cultures (Fig. 3A). The expressions of Runx2 and DSPP were increased in SP cells that had been cultured with SF2 cells, as compared with those cultured without SF2 cells (Fig. 3B). Because Runx2 and DSPP are expressed by both odontoblasts and ameloblasts, co-cultured SP and SF2 cells were separated into individual cell populations using the anti-HA antibody, which specifically recognizes SF2 cells (Fig. 3C). We found a dramatic increase in the expression level of Runx2 in SF2 cells as compared with SP cells (Fig. 3D). No epithelial marker was detected in SP cells co-cultured with SF2 cells, suggesting that the SP cells had differentiated into odontoblasts (data not shown). Runx2 is expressed in enamel matrix-secreting ameloblasts, but not in the pre-secretion stage of ameloblasts (25). Our results suggest that the SF2 cells had fully differentiated into enamel matrix-secreting ameloblasts by co-culturing with SP cells. The expression of DSPP was up-regulated in both cell types. However, in MP cells, which are fully differentiated dental papilla cells, no expression of Runx2 or DSPP was induced by co-culturing with SF2 cells (data not shown). These results indicate that epithelial and mesenchymal stem cell interactions promote individual differential states in SF2 and SP cells.

Involvement of Exogenous Factors from Dental Epithelium in DSPP Expression of SP Cells—We attempted to identify the factors in dental epithelial cells involved in SP cell differentiation by treating SF2 cells with 4% PFA to inhibit extracellular signaling, including the effects of growth factors (Fig. 4A). Ammonia treatment, through a process known as denudation, removes all cell components except the extracellular matrices and is often used for three-dimensional matrix cell culture experiments (26). DSPP expression in SP cells was partially inhibited by PFA treatment, while they retained the extracellular matrix network. This result suggests that the extracellular environment including extracellular matrices, growth factors, and cell-cell

Epithelial-Stem Cell Interactions during Dental Cell Differentiation

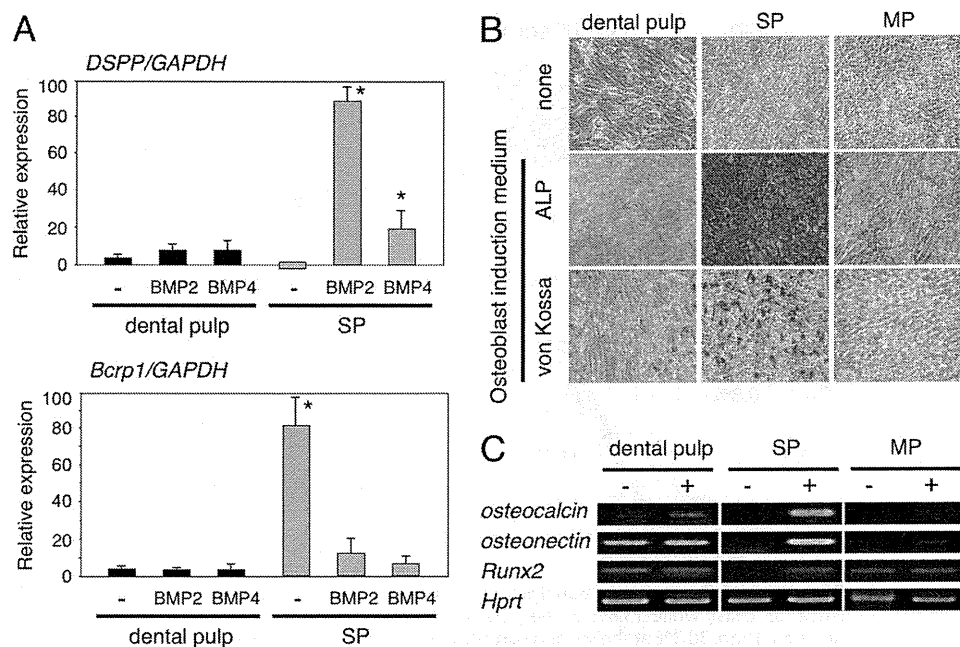


FIGURE 2. Odontoblast and osteoblast differentiation in SP cells. A, differentiation of SP cells to odontoblasts. Expression of the odontoblast marker *DSPP* and the undifferentiated mesenchymal marker *Bcrp1* in dental pulp (black bar) and SP cells (gray bar) cultured with or without BMP2 or BMP4. B, differentiation of SP cells to osteoblasts in osteoblast induction medium (*Osteogenic cond.*). ALP and von Kossa staining of dental pulp, SP, and MP cells. C, expressions of osteoblast markers in dental pulp, SP, and MP cells cultured in regular (–) or osteoblast induction medium (+). *, $p < 0.05$.

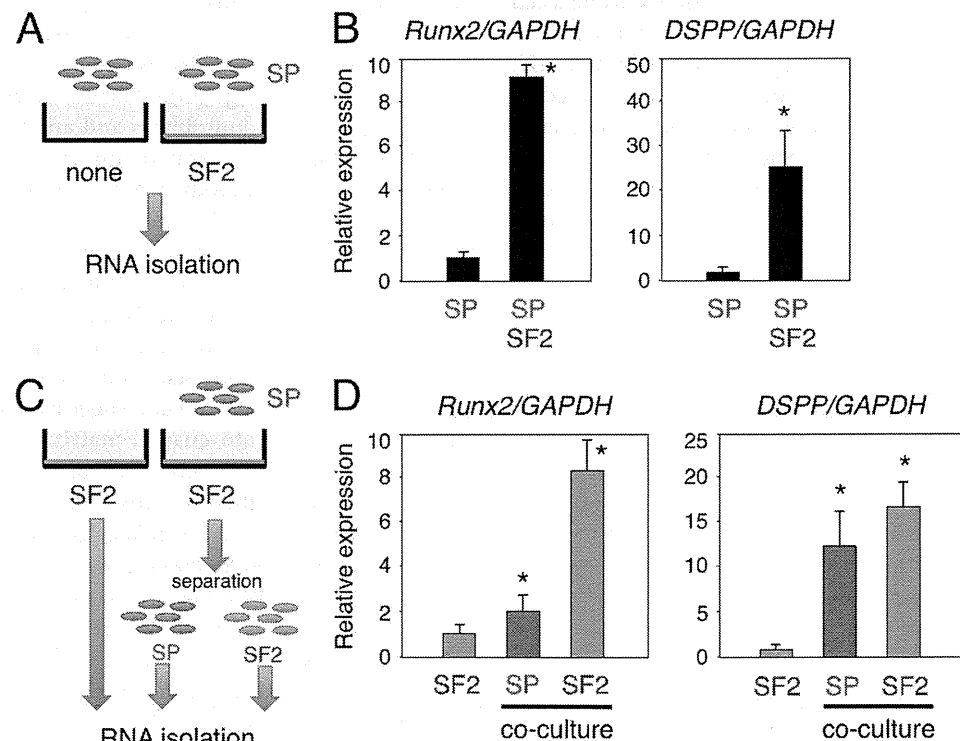


FIGURE 3. In vitro epithelial-mesenchymal interaction system using dental epithelial cells (SF2) and dental mesenchymal stem cells (SP) to promote odontogenic cell differentiation. A and C, schematic diagram of the co-culture system. B, comparisons of *Runx2* and *DSPP* gene expressions between the SP monolayer culture and SP and SF2 cell co-culture system. C, total RNA samples were separately prepared from SP and SF2 cells, using the anti-HA antibody. D, expressions of *Runx2* and *DSPP* in co-cultured SF2 (blue) and SP (red) cells. The expression level of GAPDH was used as an internal control. *, $p < 0.05$.

interaction produced by SF2 cells contributes to odontoblast induction. Denuded SF2 cells were also incapable of inducing *DSPP* expression in SP cells (Fig. 4B). Odontoblast induction of SP cells was observed in co-cultures with living SF2 cells, indicating that some types of soluble secreted molecules and mat-

rices from SF2 cells are required to induce SP cells to undergo odontogenic differentiation.

Next, we screened the factors secreted from SF2 cells that promote odontogenic cell differentiation from epithelial and mesenchymal cells using cell culture chambers, which allowed

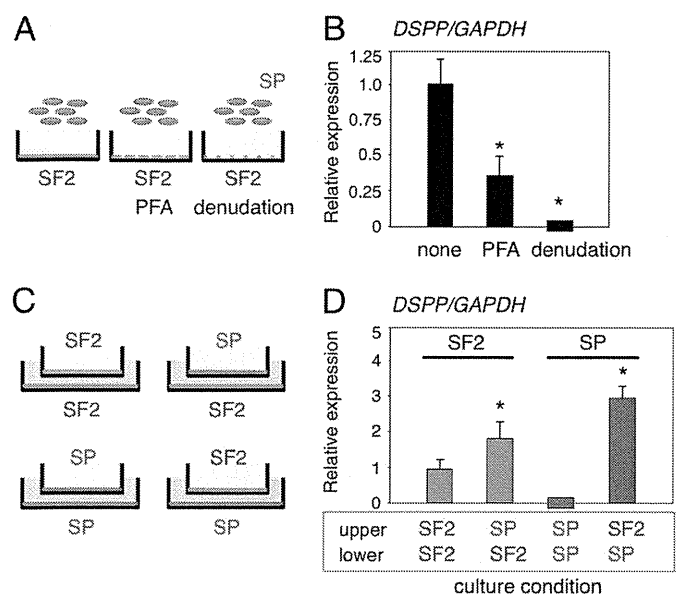


FIGURE 4. Co-culture conditions for screening of odontogenic cell differentiation using *in vitro* cell-cell interaction system. *A*, SP cells were cultured on SF2 cells in monolayers, then fixed with 4% paraformaldehyde (PFA) or treated with ammonia (denudation). *B*, DSPP expression in SP cells co-cultured under different conditions. *C*, four sets of co-culture conditions using cell chambers were analyzed. *D*, DSPP expression in SF2 cells (blue) and SP cells (red) cultured in lower dishes, with co-culture partner cells in the upper chambers. The expression level of GAPDH was used as an internal control. *, $p < 0.05$.

the factors to be secreted into cell culture medium (Fig. 4C). Heterologous combinations of SF2 and SP cells were important for promotion of DSPP expression in both types of cells. We found that co-cultures consisting of SF2 cells in the upper chamber and SP cells in the lower chamber were most effective for stimulation of DSPP gene expression in SP cells (Fig. 4D). These results suggest that secreted factors are important for induction of DSPP expression in SP cells co-cultured with dental epithelial cells.

Regulation of DSPP Expression in SP Cells via BMP2-BMP4 Crosstalk—The involvement of several different types of growth factors has been reported in epithelial-mesenchymal interactions, for example, BMPs were shown to promote dental mesenchymal cell differentiation (27). We examined the potential involvement of BMPs in SP cell differentiation by adding soluble Noggin, which antagonizes BMP activity, to cell chamber cultures that contained SP cells in the lower chambers (Fig. 5A). The presence of Noggin in culture medium resulted in down-regulation of the expression of DSPP in SP cells as compared with the control cells (Fig. 5B). Therefore, BMPs are required for induction of DSPP expression in SP cells co-cultured with dental epithelial cells. In tooth germ development, BMP4 is involved in epithelial-mesenchymal interaction, and also regulates the mesenchymal expression of *Msx1* and *Msx2*, which are important for tooth development, whereas BMP2 promotes dental mesenchymal differentiation (27). However, details regarding crosstalk between BMP2 and BMP4 in dental epithelial and mesenchymal stem cell interactions have not been elucidated. We sought to clarify the role of BMPs in these interactions by examining the expressions of BMP2 and BMP4 in SF2 and SP cells using a separated chamber assay (Fig. 5C).

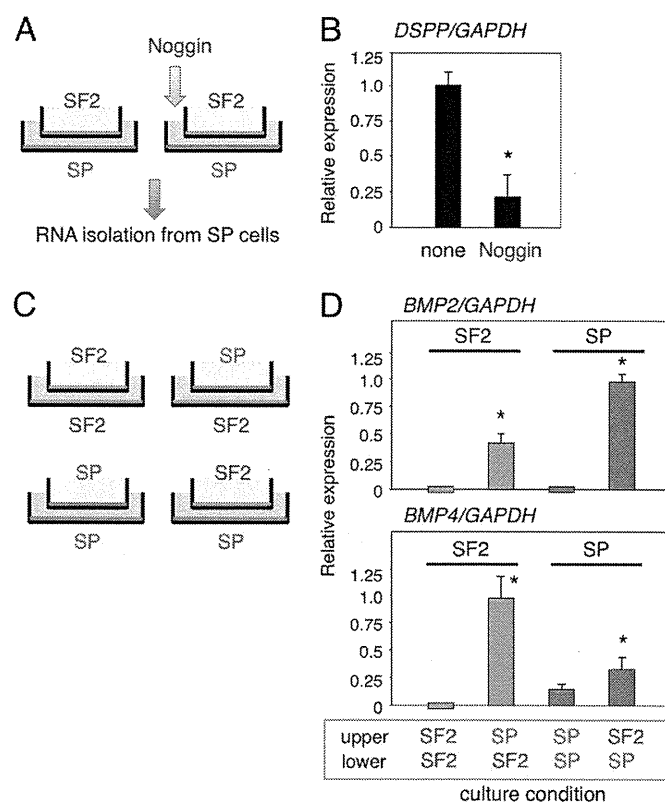


FIGURE 5. *In vitro* epithelial-mesenchymal interaction system shows that crosstalk BMP signaling is essential for odontogenic cell differentiation. *A*, total RNA was isolated from SP cells co-cultured with SF2 cells in the presence or absence of Noggin recombinant protein. *B*, DSPP expression in SP cells co-cultured with SF2 cells after blocking BMP signaling. *C*, four sets of culture conditions using cell chambers were analyzed. *D*, BMP2 and BMP4 expressions in SF2 (blue) and SP (red) cells, with co-culture partner cells in the upper chambers. *, $p < 0.05$.

The expression of BMP2 was higher in SP cells than SF2 cells under the heterologous combination culture condition, whereas BMP2 was not detected in homologous cultures (Fig. 5D). In contrast, the expression of BMP4 was higher in SF2 cells than in SP cells in the heterologous combinations (Fig. 5D). Taken together, these results suggest that the interactions between dental epithelium and dental mesenchymal stem cells induce BMP4 and BMP2, which, in turn, promote odontogenic cell differentiation via paracrine and autocrine signaling.

Optimization of Co-culture Conditions for Differentiation of iPS Cells into *Ambn*-expressing Dental Epithelial Cells—Following interaction with SF2 cells, SP cells differentiated into DSPP expressing cells, but not ameloblasts (Figs. 3, 4, and 5). This may be because SP cells are mesenchymal stem cells and committed to differentiate into mesenchyme lineage cell types. Therefore, we used mouse iPS cells to examine whether these cells can be differentiated into ameloblasts when cultured with SF2 cells. However, SF2 cells did not effectively promote their differentiation (data not shown), which may be due to the necessity of factors from differentiated dental epithelial cells for differentiation of iPS cells into ameloblasts. To test this possibility, we subcloned 25 different SF2 cell lines and examined the expression levels of the *Ambn* gene. Of these lines, the SF2-24 cell line expressed *Ambn* at the highest level (supplemental Fig. S24). Dental epithelium SF2-24 cells grew tightly together in a

Epithelial-Stem Cell Interactions during Dental Cell Differentiation

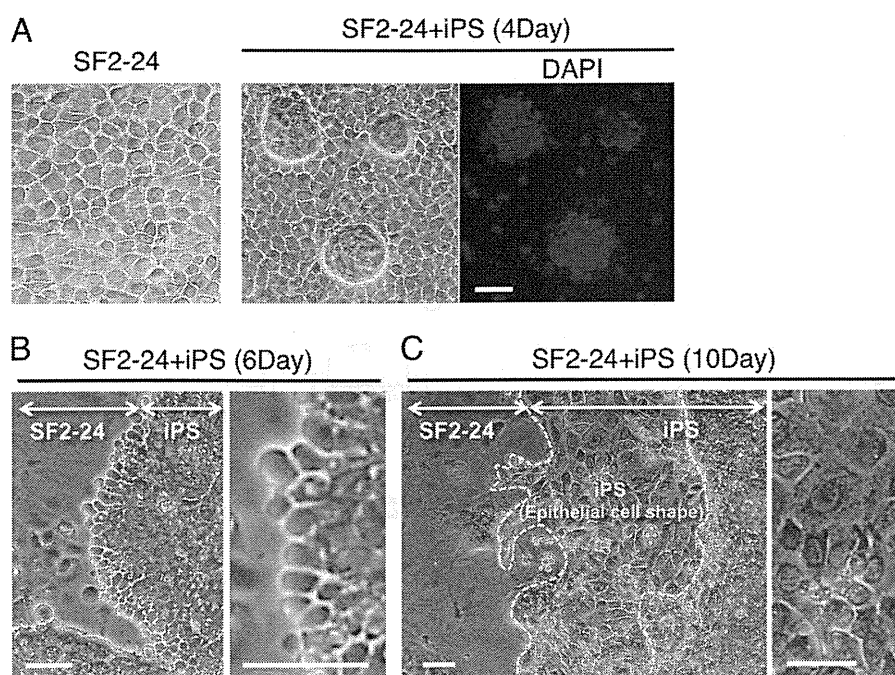


FIGURE 6. Epithelial cell shapes of iPS cells after co-culturing with SF2-24 cells. *A*, phase micrographs of monolayer SF2-24 cells and iPS cells cultured with SF2-24 feeder cells for 4 days, followed by DAPI staining. *B* and *C*, low and high magnification phase micrographs of iPS cells on MMC-treated SF2-24 feeder cells after 6 (6Day) and 10 days (10Day). Enlarged image shows a part of the iPS cells with epithelial cell shapes. *C*, epithelial cell cluster formed by iPS cell-derived epithelial cells (area within yellow dashed line). Bar, 50 μ m.

square or cuboidal shape (Fig. 6A), and expressed *Ambn* and cytokeratin-14 (CK14), but not the reprogrammed factors *Sox2*, *Klf4*, and *Oct3/4* (supplemental Fig. S3B). On the other hand, iPS cells formed colonies that expressed *Nanog* promoter-driven GFP (data not shown) as well as *Klf4*, *Sox2*, *Oct3/4*, and *Nanog*, but not *Ambn* or CK14 (supplemental Fig. S3B).

We also examined the effects of differentiation by co-culturing iPS cells with MMC-treated non-proliferating SF2-24 feeder cells (Fig. 6A). The shape of the co-cultured iPS cells was clearly rounded along the boundary of the clusters after 6 days (Fig. 6B). These cells had migrated and formed what appeared to be epithelium after 10 days (area surrounded by yellow dashed line, Fig. 6C).

The differentiation of iPS cells was then determined by RT-PCR analysis. First, we examined the specificity of mouse *Ambn* locked nucleic acid (LNA) primer sets (supplemental Fig. S4). A mouse *Ambn* LNA primer set specifically detected the mouse *Ambn* gene, but not the rat *Ambn* gene (supplemental Fig. S4A). Using this primer set, *Ambn* expression was not detected in mouse iPS cells or MEFs (supplemental Fig. S4B). Next, we examined co-culture conditions for the differentiation of iPS cells into dental epithelium (Fig. 7A). iPS cells co-cultured with MMC-treated SF2-24 cells showed a high expression of the mouse *Ambn* gene, while those co-cultured with PFA-treated or non-treated SF2-24 cells did not (Fig. 7B). SF2-24 feeder cells expressed rat *Ambn* when co-cultured with iPS cells, while that expression was reduced at 10 days (Fig. 7C).

Interestingly, expressions of the stem cell markers *Sox2*, *Oct3/4*, *Nanog*, *Fgf4*, and *Gdf3* were not changed throughout the co-culture period, because of the existence of undifferentiated iPS cells (Fig. 7C), while those of the endodermal markers *Cdx2* and *Gata6* were also not increased. Furthermore, the

mesodermal marker *Brachyury* was highly expressed in iPS cells, because of technical contamination resulting RNA extraction from MEFs used for maintenance of the iPS cells, and then gradually decreased over time. We also observed increased expressions of the mouse ameloblast markers *Ambn* and *Enamelin* (*Enam*), as well as the epithelial markers CK14 and p63, in iPS cells after 7 and 10 days (Fig. 7C). Furthermore, the expression of *epiprofin/Sp6*, a transcription factor highly expressed in dental epithelium (28), was increased in those cells (supplemental Fig. S5). A similar expression pattern was observed in co-cultured iPS cells separated from SF2-24 cells using the anti-HA antibody (data not shown).

Differentiation of iPS Cells into *Ambn*-expressing Dental Epithelial Cells—We then examined the protein expression of *Ambn* in iPS cells using immunostaining. Approximately 95% of the epithelial-like cells were positive for *Ambn* (Fig. 8A), while the immunofluorescence intensity of *Ambn* was stronger in iPS cells than in SF2-24 cells (Fig. 8B). Therefore, mouse iPS cells differentiated into dental epithelium, but not into endodermal or mesodermal cells.

We attempted to identify the factors involved in differentiation of iPS cells into dental epithelium by culturing with MEFs in medium conditioned by SF2-24 cell cultures (Fig. 9A). Culturing with SF2-24 condition medium induced the expression of *Ambn* in iPS cells, indicating an involvement of soluble factors including growth factors, and extracellular matrices derived from SF2-24 cells (Fig. 9B). Next, we examined the effect of *Ambn* on differentiation of iPS cells into dental epithelial cells. Expression vectors for the full-length (AB1), C-terminal (AB2), and N-terminal (AB3) half of *Ambn* (Fig. 9C) were separately transfected into *Ambn* low-expressing cells (SF2-7), then conditioned media from those cells or recombinant *Ambn*

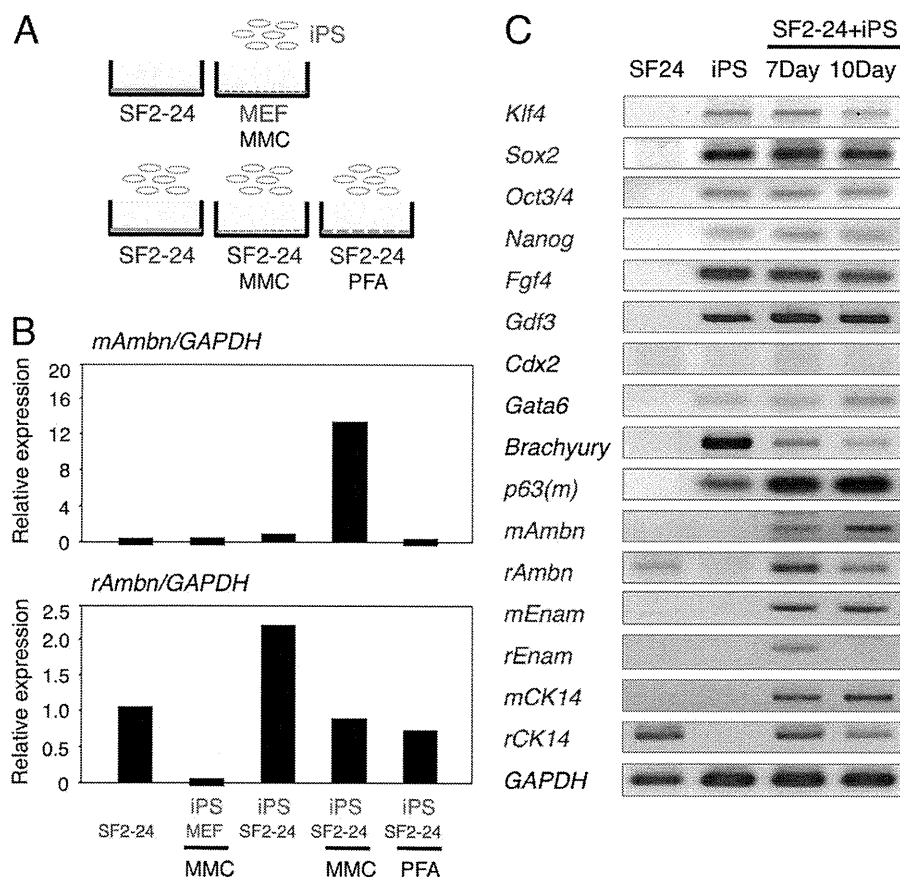


FIGURE 7. **Effects of culture conditions on ameloblast induction of iPS cells.** A, iPS cells were co-cultured with SF2-24 cells, MMC-treated (MMC) MEFs, MMC-treated SF2-24 cells or PFA-treated SF2-24 cells. B, Ambn expression in mouse iPS (upper panel) and rat-derived SF2-24 (bottom panel) cells in different co-culture conditions for 10 days. C, time course analysis of gene expressions of stem cell (blue), endo/mesoderm (black), and ameloblast (red) markers in iPS cells co-cultured with SF2-24 cells for 7 (7Day) and 10 days (10Day).

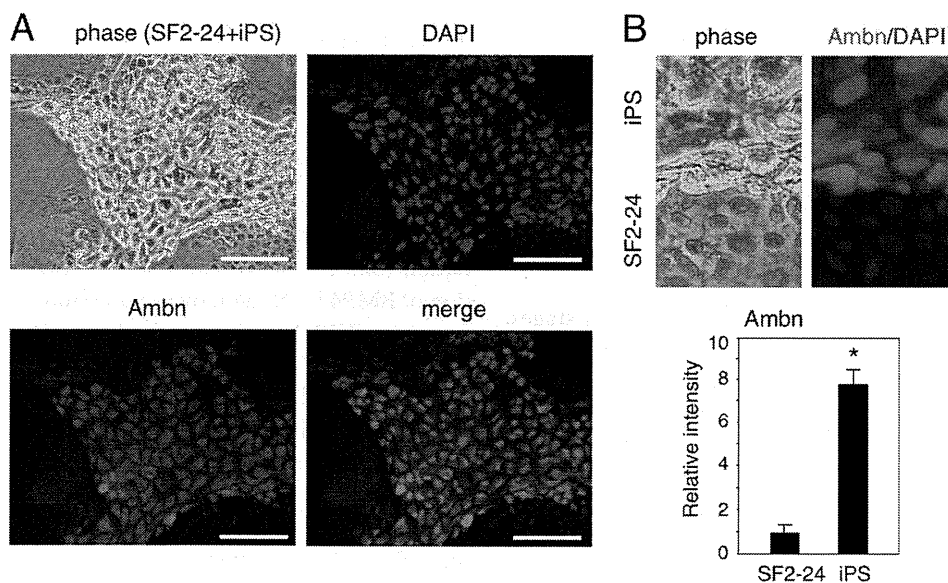


FIGURE 8. **Expression of Ambn, an ameloblast specific protein, in iPS cells co-cultured with SF2-24 cells.** A, phase micrographs of iPS cell colonies cultured with mitomycin C-treated SF2-24 cells. Hoechst staining (blue), Ambn staining (red), and merged images. B, high magnifications of phase and merged images in A. Bottom panel, relative expression levels of Ambn protein in SF2-24 and iPS cells cultured in ameloblast induction system. *, $p < 0.05$; Bar, 100 μ m.

proteins (AB1, -2, or -3) were added to cultures of iPS cells. Conditioned media from SF2-24 cells and full-length AMBN-expressing cells, but not from other transfectants or recombinant Ambn proteins, induced Ambn expression in iPS cells

(Fig. 9D), indicating that Ambn may be necessary for differentiation of iPS cells into dental epithelium. Previously, we showed that neurotrophic factor NT-4 is important for the differentiation of ameloblasts (29). To examine the effect of NT-4

Epithelial-Stem Cell Interactions during Dental Cell Differentiation

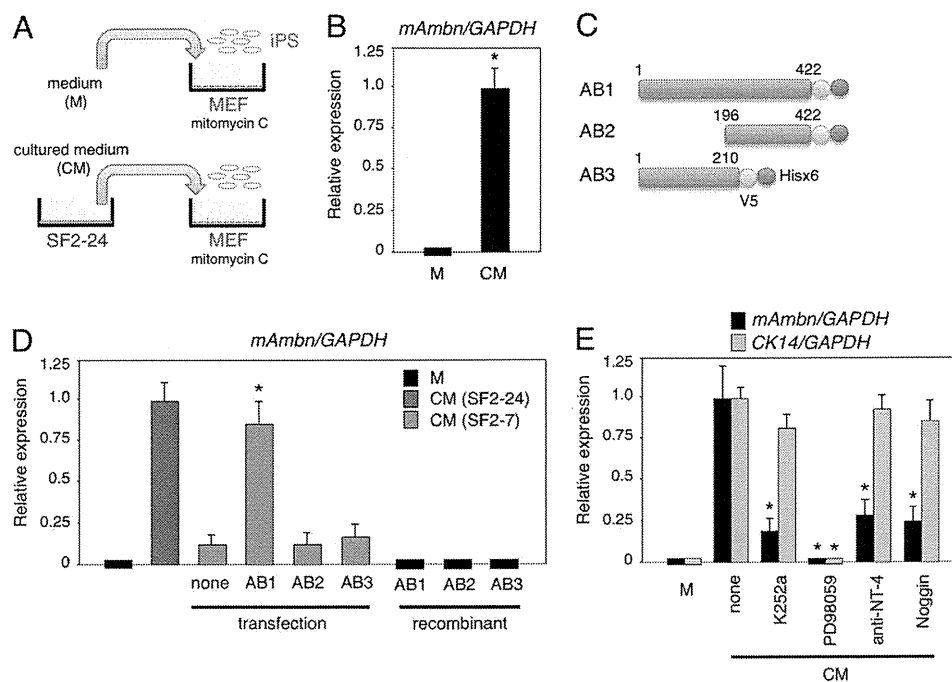


FIGURE 9. Promotion of ameloblast induction of iPS cells using conditioned SF2-24 cells. A, iPS cells were cultured on mitomycin C-treated MEFs in iPS cell culture medium supplemented with (CM) or without (M) conditioned medium from SF2-24 cells. B, expression of mouse *Ambn* gene in iPS cells cultured in iPS cell culture medium supplemented with (CM) or without (M) conditioned medium from SF2-24 cells. C, creation of *Ambn* deletions. All recombinant *Ambn* proteins have V5 and His tags at the C terminus. D, expression of mouse *Ambn* gene in iPS cells cultured in iPS cell culture medium supplemented with (CM) or without (M) conditioned medium from SF2-24 cells, recombinant *Ambn*-expressing SF2-7 cells or recombinant *Ambn* proteins. *, $p < 0.05$ (compared with non-transfected SF2-7 cells). E, expression of mouse *Ambn* and *CK14* genes in iPS cells cultured in SF2-24 conditioned medium supplemented with K252a, PD98059, anti-NT-4, or Noggin. *, $p < 0.05$ (compared with CM only).

on dental epithelial cell differentiation by iPS cells, we analyzed the expressions of *Ambn* and *CK14* in iPS cells cultured with SF2-24-conditioned medium in the presence of K252a (inhibitor of neurotrophic receptor Trk), PD98059 (MEK inhibitor), anti-NT-4 neutralizing antibody, or Noggin (BMP antagonist). K252a, PD98059, anti-NT-4, and Noggin each inhibited the expression of *Ambn* in iPS cells. Furthermore, *CK14* expression in iPS cells was not inhibited by K252a, anti-NT-4, or Noggin (Fig. 9E). These results indicate that NT-4 and BMP signaling are important for differentiation into dental epithelial cells, but not *CK14*-positive epithelial cells.

DISCUSSION

Tooth development progresses through a number of stages, and the differentiation of dentin matrix-secreting odontoblasts and enamel matrix-producing ameloblasts results in formation of the crown. Ameloblasts and odontoblasts are central cell types involved in tooth development. In developing molars, restricted dental mesenchymal cells interact with the inner dental epithelium through the matrix and differentiate into odontoblasts. In the present study, we established an SP cell line from dental papilla mDP cells using cell sorting with Hoechst staining. SP cells are known to retain multipotency characteristics and can differentiate into various cell types, such as odontoblasts, osteoblasts, adipocytes, and neural cells. Our method for obtaining multipotent SP cells from a single cell line may be useful for development of novel therapeutic strategies that aim at regeneration of oral tissues.

Our co-culture assay of SP cells with dental epithelial cells showed that dental epithelial cells promote SP cell differentia-

tion into DSPP-expressing cells via BMP2 and BMP4, which are secreted from dental epithelial cells (Fig. 5B, 5D, and 10A). Because BMP2 is not highly expressed in dental epithelium, BMP4 may be the dominant signaling regulator during odontoblast differentiation. In the early stages of tooth development, BMP4 is expressed in dental epithelium and induces the transcription factor *Msx1* (30). The expression of DSPP is induced via the BMP signaling pathway in cooperation with *Runx2*, *Dlx5*, and *Msx1* in undifferentiated mesenchymal cells (31). Previously, a bead soak assay of mandibular organ culture showed that BMP4 induced dental mesenchymal cell differentiation (32). Also, a transgenic approach revealed that inhibition of BMP4 by Noggin overexpression, driven by a keratin 14 promoter (K14-Noggin), resulted in the absence of all molars in the mandible. This indicates that BMP4 is essential for tooth bud formation by inducing dental mesenchymal cells (33). As demonstrated, in the present study odontoblastic differentiation of SP cells is completely disturbed by the blocking of BMP signaling. Thus, our finding strongly support the notion that BMP4 signaling is a key factor in induction of dental mesenchymal cells and their differentiation.

Differential synchronization between dental epithelial and mesenchymal cells has been observed during tooth development. Dental epithelial and mesenchymal cells are separated by a basement membrane, which is an essential regulator for epithelial-mesenchymal interaction (34). Both crown and root odontoblasts are induced by interactions with epithelial cells, such as those of the inner dental epithelium, epithelial rest, and epithelial diaphragm (35). Similar to *in vivo* situations, physical

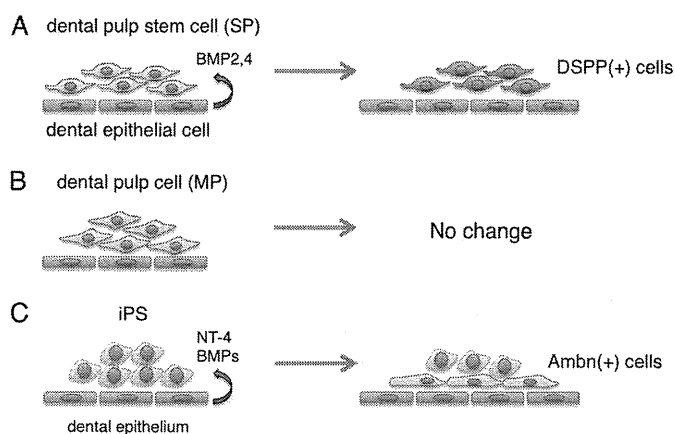


FIGURE 10. Proposed models of odontogenic induction from dental mesenchymal stem cells and iPS cells by co-culturing with dental epithelial cells. *A*, dental epithelial cells induce DSPP-expressing odontoblasts from SP cells. *B*, no odontogenic induction was observed in differentiated (MP) cells co-cultured with dental epithelial cells. *C*, dental epithelial cells induce Ambn-expressing ameloblasts from iPS cells.

cell attachment of dental epithelial cells was not required for odontogenic induction of SP cells in our experiments, indicating that soluble factors including BMPs are important for odontogenic induction by dental epithelial cells in culture. We also found that MP cells from dental papilla did not differentiate into DSPP-expressing cells, indicating that epithelial-mesenchymal interactions are important for cell fate determination of dental pulp stem cells, but not for differentiated dental pulp cells (Fig. 10, *A* and *B*). It was recently reported that Ambn protein, or a synthetic peptide based on the N-terminal region of the Ambn protein, induced osteoblastic cell differentiation (36). In addition to BMPs, Ambn may also be one of the factors involved in the odontogenic induction process, because the sharing of signaling pathways underlies the mechanism of odontoblastic and osteoblastic induction.

Ameloblasts secrete enamel-specific extracellular matrices including Ambn, which are lost upon tooth eruption. This makes it impossible to repair or replace damaged enamel in an erupted tooth. Therefore, identifying alternative sources of these cells becomes important. Bone marrow-derived cells can give rise to different types of epithelial cells. In mixed cultures with *c-Kit*⁺-enriched bone marrow cells, embryonic dental epithelial cells, and dental mesenchyme, bone marrow cells might be reprogrammed to give rise to ameloblast-like cells (37). Our strategy to create ameloblasts from mouse iPS cells may have direct application in tooth regeneration. We succeeded in establishing a co-culture system using cells derived from two different species, mouse iPS cells and rat derived enamel matrix secreting ameloblasts. This is the first demonstration of differentiation of iPS cells into ameloblasts through interactions with dental epithelium (Fig. 10C). However, a set of stem cell markers was continuously expressed in iPS cells after 7 days of co-culturing (Fig. 7C), indicating that a portion of the iPS cells had differentiated into enamel-secreting ameloblasts and some still retained stem cell potential. Thus, the efficacy of iPS cell differentiation into ameloblasts by enamel-secreting ameloblasts feeder cells must be improved prior to for clinical application.

A number of factors are thought to give iPS cells the capacity for direct or indirect differentiation into ameloblasts. Possible direct effectors include gap junctions, intercellular binding molecules, adhesion factors, and extracellular matrices secreted by dental epithelium. Growth factors might also be involved, because conditioned medium from SF2-24 cells induced Ambn expression in iPS cells. Ambn is also a candidate factor for dental cell differentiation of iPS cells, as SF2 cells expressing low levels of Ambn did not induce differentiation of iPS cells. Furthermore, overexpression of full-length Ambn in cells expressing low levels of Ambn induced iPS cells into ameloblast-like differentiation (Fig. 9D). Ambn has diverse functions in various cellular physiologies, such as cell growth, differentiation, cell polarization, and attachment, though the detailed mechanisms of Ambn signaling require additional investigation. Ambn-null mice display severe enamel hypoplasia due to impaired dental epithelial cell proliferation, polarization, and differentiation into ameloblasts, as well as loss of cell attachment activity with immature enamel matrix (2). These results suggest that Ambn, especially full-length, is necessary for both *in vivo* and *in vitro* ameloblast differentiation.

There were differences in cell lineage determination of the dental pulp stem cells and iPS cells when co-cultured with dental epithelial cells. RT-PCR analysis showed that co-culturing induced SP cells to form odontoblastic cells, whereas iPS cells were induced to form ameloblastic cells. In addition, the expression of Brachyury, a mesodermal marker, in iPS cells was down-regulated by co-culturing with SF2-24 cells (Fig. 7C). Conversely, expressions of the epithelial markers p63 and CK14, as well as the dental epithelial marker epiprofin/Sp6 were up-regulated (Fig. 7C, supplemental Fig. S5) (28). These results suggest that the cell lineage of the iPS cells in our co-culturing system was effectively guided into an epithelial cell lineage. It has been reported that the default cell lineage of ES cells is the ectodermal cells, except when cultured in the presence of BMP antagonists (38, 39). Because BMPs promote ectodermal differentiation of ES cells, the expression of BMP observed in SF2 cells (Fig. 5D) may also contribute to dental epithelial cell differentiation of iPS cells. A previous our reported that NT-4 induced Ambn expression in dental epithelium, while NT-4 knock-out mice showed delayed expression of enamel matrices in the early stage of ameloblast differentiation (29). In the present study, the presence of the anti-NT-4 neutralizing antibody or Noggin in conditioned medium from SF2-24 cells inhibited Ambn expression, but not that of CK14 (Fig. 9E). On the other hand, SP cells strongly expressed the endogenous Sox2 protein, one of the reprogramming factors involved in generation of iPS cells (data not shown). Recently, iPS cells were generated from human dental pulp cells with a high level of efficiency in comparison to dermal fibroblasts, possibly due to a high expression level of Sox2 in dental pulp stem cells. However, additional reprogramming factors are required for creation of iPS cells from dental pulp cells. Thus, SP cells themselves did not have the same degree of multipotency as seen with ES and iPS cells. SP cells are considered to be mesenchymal stem cells that originate from dental pulp cells, which are derived from cranial neural crest cells. Neural crest cells can differentiate into several different cell lineages, such as neuron, glia, melanocyte,

Epithelial-Stem Cell Interactions during Dental Cell Differentiation

osteoblast, chondrocyte, and odontoblast cells (40, 41). We believe that SP cells are not able to gain multipotency beyond the potential of neural crest cells. Thus, SP cells preserve some degree of multipotency that is different in an undifferentiated state as compared with ES and iPS cells. In co-cultures with SF2-24 cells, SP cells did not differentiate into ameloblasts, whereas iPS cells did (Fig. 10). Comparative analysis between SP and iPS cells is essential to clarify the mechanisms involved in directional cell fate determination.

In this study, we sought to clarify the role of dental epithelium and stem cell interactions by culturing rat dental epithelium with mouse iPS cells and SP cells. Rodent incisors grow throughout the lifespan of the animal by maintaining stem cells in the cervical loop, located at the end of incisor. A dental epithelial cell niche also exists in the cervical loop of the incisor. Analysis of gene knock-out mice for epiprofin/Sp6, an essential transcription factor for dental epithelial cell differentiation and enamel formation, has revealed that supernumerary teeth are formed by interactions between dental mesenchyme and undifferentiated dental epithelium (4, 42). In addition, those studies showed continuous signals from dental epithelial cells of mutant mice induced the continued differentiation of dental mesenchymal cells into odontoblasts (4, 42). Together these findings suggest that dental epithelial cells can induce dental mesenchymal cells to differentiate into odontoblasts. Therefore, rat dental epithelial cells may provide an *in vitro* niche environment for surrounding mouse iPS cells and SP cells. Elucidation of the mechanism of cell fate determination by dental epithelial cells may facilitate development of novel therapeutic approaches for regenerative dentistry.

REFERENCES

1. Thesleff, I. (2003) Epithelial-mesenchymal signaling regulating tooth morphogenesis. *J. Cell Sci.* **116**, 1647–1648
2. Fukumoto, S., Kiba, T., Hall, B., Iehara, N., Nakamura, T., Longenecker, G., Krebsbach, P. H., Nanci, A., Kulkarni, A. B., and Yamada, Y. (2004) Ameloblastin is a cell adhesion molecule required for maintaining the differentiation state of ameloblasts. *J. Cell Biol.* **167**, 973–983
3. Yuasa, K., Fukumoto, S., Kamasaki, Y., Yamada, A., Fukumoto, E., Kanaoka, K., Saito, K., Harada, H., Arikawa-Hirasawa, E., Miyagoe-Suzuki, Y., Takeda, S., Okamoto, K., Kato, Y., and Fujiwara, T. (2004) Laminin $\alpha 2$ is essential for odontoblast differentiation regulating dentin sialoprotein expression. *J. Biol. Chem.* **279**, 10286–10292
4. Nakamura, T., de Vega, S., Fukumoto, S., Jimenez, L., Unda, F., and Yamada, Y. (2008) Transcription factor epiprofin is essential for tooth morphogenesis by regulating epithelial cell fate and tooth number. *J. Biol. Chem.* **283**, 4825–4833
5. Fisher, L. W., and Fedarko, N. S. (2003) Six genes expressed in bones and teeth encode the current members of the SIBLING family of proteins. *Connect. Tissue Res.* **44**, Suppl. 1, 33–40
6. Takahashi, K., Tanabe, K., Ohnuki, M., Narita, M., Ichisaka, T., Tomoda, K., and Yamanaka, S. (2007) Induction of pluripotent stem cells from adult human fibroblasts by defined factors. *Cell* **131**, 861–872
7. Lewitzky, M., and Yamanaka, S. (2007) Reprogramming somatic cells towards pluripotency by defined factors. *Curr. Opin. Biotechnol.* **18**, 467–473
8. Xu, D., Alipio, Z., Fink, L. M., Adcock, D. M., Yang, J., Ward, D. C., and Ma, Y. (2009) Phenotypic correction of murine hemophilia A using an iPS cell-based therapy. *Proc. Natl. Acad. Sci. U.S.A.* **106**, 808–813
9. Hanna, J., Wernig, M., Markoulaki, S., Sun, C. W., Meissner, A., Cassady, J. P., Beard, C., Brambrink, T., Wu, L. C., Townes, T. M., and Jaenisch, R. (2007) Treatment of sickle cell anemia mouse model with iPS cells generated from autologous skin. *Science* **318**, 1920–1923
10. Soldner, F., Hockemeyer, D., Beard, C., Gao, Q., Bell, G. W., Cook, E. G., Hargus, G., Blak, A., Cooper, O., Mitalipova, M., Isacson, O., and Jaenisch, R. (2009) Parkinson disease patient-derived induced pluripotent stem cells free of viral reprogramming factors. *Cell* **136**, 964–977
11. Okita, K., Ichisaka, T., and Yamanaka, S. (2007) Generation of germline-competent induced pluripotent stem cells. *Nature* **448**, 313–317
12. So, K. H., Han, Y. J., Park, H. Y., Kim, J. G., Sung, D. J., Bae, Y. M., Yang, B. C., Park, S. B., Chang, S. K., Kim, E. Y., and Park, S. P. (2010) *Int. J. Cardiol.* **153**, 277–285
13. Yoshida, Y., and Yamanaka, S. (2011) *J. Mol. Cell Cardiol.* **50**, 327–332
14. Miura, M., Gronthos, S., Zhao, M., Lu, B., Fisher, L. W., Robey, P. G., and Shi, S. (2003) SHED: stem cells from human exfoliated deciduous teeth. *Proc. Natl. Acad. Sci. U.S.A.* **100**, 5807–5812
15. Gronthos, S., Mankani, M., Brahimi, J., Robey, P. G., and Shi, S. (2000) Postnatal human dental pulp stem cells (DPSCs) *in vitro* and *in vivo*. *Proc. Natl. Acad. Sci. U.S.A.* **97**, 13625–13630
16. Shi, S., Bartold, P. M., Miura, M., Seo, B. M., Robey, P. G., and Gronthos, S. (2005) The efficacy of mesenchymal stem cells to regenerate and repair dental structures. *Orthod. Craniofac. Res.* **8**, 191–199
17. Goodell, M. A., Brose, K., Paradis, G., Conner, A. S., and Mulligan, R. C. (1996) Isolation and functional properties of murine hematopoietic stem cells that are replicating *in vivo*. *J. Exp. Med.* **183**, 1797–1806
18. Zhou, S., Schuetz, J. D., Bunting, K. D., Colapietro, A. M., Sampath, J., Morris, J. J., Lagutina, I., Grosfeld, G. C., Osawa, M., Nakauchi, H., and Sorrentino, B. P. (2001) The ABC transporter Bcrp1/ABCG2 is expressed in a wide variety of stem cells and is a molecular determinant of the side-population phenotype. *Nat. Med.* **7**, 1028–1034
19. Li, L., Kwon, H. J., Harada, H., Ohshima, H., Cho, S. W., and Jung, H. S. (2011) Expression patterns of ABCG2, Bmi-1, Oct-3/4, and Yap in the developing mouse incisor. *Gene Expr. Patterns* **11**, 163–170
20. Nam, H., and Lee, G. (2009) Identification of novel epithelial stem cell-like cells in human deciduous dental pulp. *Biochem. Biophys. Res. Commun.* **386**, 135–139
21. Yan, X., Qin, H., Qu, C., Tuan, R. S., Shi, S., and Huang, G. T. (2010) iPS cells reprogrammed from human mesenchymal-like stem/progenitor cells of dental tissue origin. *Stem. Cells Dev.* **19**, 469–480
22. Yokoi, T., Saito, M., Kiyono, T., Iseki, S., Kosaka, K., Nishida, E., Tsubakimoto, T., Harada, H., Eto, K., Noguchi, T., and Teranaka, T. (2007) Establishment of immortalized dental follicle cells for generating periodontal ligament *in vivo*. *Cell Tissue Res.* **327**, 301–311
23. Klotz, O. (1905) Studies upon calcareous degeneration: I. The process of pathological calcification. *J. Exp. Med.* **7**, 633–674
24. Sonoda, A., Iwamoto, T., Nakamura, T., Fukumoto, E., Yoshizaki, K., Yamada, A., Arakaki, M., Harada, H., Nonaka, K., Nakamura, S., Yamada, Y., and Fukumoto, S. (2009) Critical role of heparin binding domains of ameloblastin for dental epithelium cell adhesion and ameloblastoma proliferation. *J. Biol. Chem.* **284**, 27176–27184
25. Chen, S., Gu, T. T., Sreenath, T., Kulkarni, A. B., Karsenty, G., and MacDougall, M. (2002) Spatial expression of Cbfa1/Runx2 isoforms in teeth and characterization of binding sites in the *DSPP* gene. *Connect. Tissue Res.* **43**, 338–344
26. Cukierman, E., Pankov, R., Stevens, D. R., and Yamada, K. M. (2001) Taking cell-matrix adhesions to the third dimension. *Science* **294**, 1708–1712
27. Nakashima, M. (1994) Induction of dentin formation on canine amputated pulp by recombinant human bone morphogenetic proteins (BMP)-2 and -4. *J. Dent. Res.* **73**, 1515–1522
28. Nakamura, T., Unda, F., de-Vega, S., Vilaxa, A., Fukumoto, S., Yamada, K. M., and Yamada, Y. (2004) The Krüppel-like factor epiprofin is expressed by epithelium of developing teeth, hair follicles, and limb buds and promotes cell proliferation. *J. Biol. Chem.* **279**, 626–634
29. Yoshizaki, K., Yamamoto, S., Yamada, A., Yuasa, K., Iwamoto, T., Fukumoto, E., Harada, H., Saito, M., Nakasima, A., Nonaka, K., Yamada, Y., and Fukumoto, S. (2008) Neurotrophic factor neurotrophin-4 regulates ameloblastin expression via full-length TrkB. *J. Biol. Chem.* **283**, 3385–3391
30. Chen, Y., Bei, M., Woo, I., Satokata, I., and Maas, R. (1996) Msx1 controls inductive signaling in mammalian tooth morphogenesis. *Development* **122**, 3035–3044

Epithelial-Stem Cell Interactions during Dental Cell Differentiation

31. Cho, Y. D., Yoon, W. J., Woo, K. M., Baek, J. H., Park, J. C., and Ryoo, H. M. (2010) The canonical BMP signaling pathway plays a crucial part in stimulation of dentin sialophosphoprotein expression by BMP-2. *J. Biol. Chem.* **285**, 36369–36376
32. Vainio, S., Karavanova, I., Jowett, A., and Thesleff, I. (1993) Identification of BMP-4 as a signal mediating secondary induction between epithelial and mesenchymal tissues during early tooth development. *Cell* **75**, 45–58
33. Plikus, M. V., Zeichner-David, M., Mayer, J. A., Reyna, J., Bringas, P., Thewissen, J. G., Snead, M. L., Chai, Y., and Chuong, C. M. (2005) Morphoregulation of teeth: modulating the number, size, shape and differentiation by tuning Bmp activity. *Evol. Dev.* **7**, 440–457
34. Thesleff, I., and Hurmerinta, K. (1981) Tissue interactions in tooth development. *Differentiation* **18**, 75–88
35. Ten Cate, A. R. (1996) The role of epithelium in the development, structure and function of the tissues of tooth support. *Oral Dis.* **2**, 55–62
36. Iizuka, S., Kudo, Y., Yoshida, M., Tsunematsu, T., Yoshiko, Y., Uchida, T., Ogawa, I., Miyauchi, M., and Takata, T. (2011) Ameloblastin regulates osteogenic differentiation by inhibiting Src kinase via cross talk between integrin β 1 and CD63. *Mol. Cell Biol.* **31**, 783–792
37. Hu, B., Unda, F., Bopp-Kuchler, S., Jimenez, L., Wang, X. J., Haikel, Y., Wang, S. L., and Lesot, H. (2006) Bone marrow cells can give rise to ameloblast-like cells. *J. Dent. Res.* **85**, 416–421
38. Chang, C., and Hemmati-Brivanlou, A. (1998) Cell fate determination in embryonic ectoderm. *J. Neurobiol.* **36**, 128–151
39. Muñoz-Sanjuan, I., and Brivanlou, A. H. (2002) Neural induction, the default model and embryonic stem cells. *Nat. Rev. Neurosci.* **3**, 271–280
40. Baroffio, A., Dupin, E., and Le Douarin, N. M. (1991) Common precursors for neural and mesectodermal derivatives in the cephalic neural crest. *Development* **112**, 301–305
41. Sieber-Blum, M., and Cohen, A. M. (1980) Clonal analysis of quail neural crest cells: they are pluripotent and differentiate *in vitro* in the absence of noncrest cells. *Dev. Biol.* **80**, 96–106
42. Nakamura, T., Fukumoto, S., and Yamada, Y. (2011) Review: diverse function of epiprofin in tooth development. *J. Oral Biosci.* **53**, 22–30

Expert Opinion

1. Introduction
2. Development processes in periodontal tissue
3. Regeneration therapies for PDL defects
4. Novel approaches to periodontal tissue regeneration using ECM administration therapy
5. Conclusions
6. Expert opinion

informa
healthcare

Extracellular matrix administration as a potential therapeutic strategy for periodontal ligament regeneration

Masahiro Saito[†] & Takashi Tsuji

[†]*Tokyo University of Science, Faculty of Industrial Science and Technology, Noda, Japan*

Introduction: The current strategies employed for the treatment of connective tissue disease include the application of stem cells, the use of functional molecules that can reorganize tissue integrity and cellular activities to recover connective tissue function. Approaches to the regeneration of periodontal tissue, which is the tooth-supporting connective tissue, have made some progress recently and provide a useful experimental model for the evaluation of future strategies to treat connective tissue diseases such as periodontal disease.

Areas covered: The ultimate goal of periodontal tissue regeneration is to reconstruct the ligament structure that will sustain the required mechanical force to connect with mineralized tissues such as cementum and alveolar bone. In this review, we discuss the proposed use of extracellular matrix (ECM) administration therapy as an additional therapeutic strategy to stem cell transplantation and cytokine administration in the current field of periodontal tissue regeneration therapy.

Expert opinion: Although various available tissue engineering technologies can now achieve periodontal tissue regeneration, ECM administration therapy is likely to play an essential future role in the development and regeneration of periodontal tissue and attenuate the signaling events that mediate tissue degradation. Hence, ECM administration could serve as a novel technology in periodontal tissue regeneration and also as a viable approach to alleviating connective tissue disorders such as Marfan's syndrome.

Keywords: connective tissue, microfibril, PDL, regenerative therapy

Expert Opin. Biol. Ther. (2012) 12(3):299-309

1. Introduction

Periodontal tissue is a tooth-supporting tissue comprising periodontal ligament (PDL), cementum and alveolar bone. This tissue thereby plays an important role in the maintenance of the occlusion system. Among the components of periodontal tissue, the PDL consists mainly of an extracellular matrix (ECM) that provides the physical properties to withstand mechanical stress in cooperation with the cementum and alveolar bone. Dysfunction of the PDL occurs as a result of periodontal disease, an inflammatory disorder involving the irreversible destruction of periodontal tissues and requiring the regeneration of PDL as a treatment for recovering occlusion function [1,2]. Periodontal disease is caused by pathogenic microflora including *Porphyromonas gingivalis*, *Tannerella forsythia* and *Treponema denticola*, and the resulting inflammation extends deep into the periodontal tissue and causes the loss of PDL, cementum and alveolar bone [3]. Chronic periodontal disease is the most common form of this disorder, showing a prevalence rate of > 90% in adults

Article highlights.

- Periodontal tissue regeneration aims to reconstruct the ligament structures in the tooth-supporting connective tissue.
- Periodontal ligament (PDL) stem cells can be used to reconstitute the PDL structure, including extracellular components.
- PDL stem cells (PDLSCs) express mesenchymal stem cell markers STRO-1 and CD146/MUC18 and show a similar phenotype to dental follicle stem cells (DFSCs).
- PDL cell sheets may induce periodontal regeneration, including reforming the PDL and cementum, and could provide an *in vivo* treatment for periodontal disease.
- The local application of human recombinant cytokines such as fibroblast growth factor (FGF)-2, platelet-derived growth factor (PDGF), bone morphogenetic protein (BMP)-2 and TGF- β stimulates and promotes the regeneration of periodontal tissues in animal models.
- Fibrillin-1 microfibril network is also important for PDL function and maintaining connective tissue integrity. Targeting the extracellular matrix (ECM) and fibrillin-1 microfibrils may offer a new administration therapy for periodontal disease.

This box summarizes key points contained in the article.

over 60 years of age [4]. Furthermore, this disorder is the major cause of tooth loss in adults of over 40 years and its more severe forms has a worldwide prevalence of up to 20% according to the World Health Organization [5]. Blocking the progression of periodontal disease has been achieved by mechanically removing bacterial biofilm with conventional periodontal and/or surgical treatments. These treatments can reduce the destruction of periodontal tissue and diminish inflammation in the affected region. However, achieving adequate periodontal tissue regeneration remains a problem, particularly in cases where the disease has caused large defects in the periodontal tissue.

The current advances in future regenerative therapies have been influenced by many previous studies of embryonic development, stem cell biology and tissue engineering technologies [6-9]. To restore the partial loss of organ functions and to repair damaged tissues, attractive concepts that have emerged in regenerative therapy is stem cell transplantation into various tissues and organs [10] and cytokine therapy, which has the potential to induce the activation and differentiation of tissue stem/progenitor cells [11]. Tooth tissue stem cells and the cytokine network that regulates tooth development, and dental tissue cell growth and differentiation, have been well characterized at the molecular level [12,13]. The regeneration of periodontal tissues is being made clinically possible by the transplantation of mesenchymal stem cells which can differentiate into PDL cells, cementoblasts and osteoblasts, or through the local application of cytokines to stimulate the proliferation and differentiation of these stem cells [14-17]. Although these therapies are effective and contribute to periodontal tissue repair, these interventions will likely be improved by an enhanced understanding of the

development of periodontal tissues, particularly those involved in the formation of PDL, cementum and alveolar bone.

The ECM is a biologically active molecule composed of a complex mixture of macromolecules that, in addition to serving a structural function, profoundly affect the cellular physiology of an organism [18]. Previous findings have revealed that ECM components including type I collagen, type III collagen, lumican, decorin, periostin, f-spondin, tenascin-N and PLAP1/aspirin are highly expressed during PDL formation [19,20]. Since the ECM is regulated in a tissue-specific manner, these structures could enhance periodontal regeneration by promoting the differentiation of cells required for the synthesis of PDL, bone and cementum [21,22]. Among the ECM formations in the PDL, fibrillin-1, a major component of the microfibrils that regulate tissue integrity and elasticity, has been shown to contribute to the formation and maintenance of this ligament. An abnormal PDL structure in association with the progressive destruction of microfibrils has been observed in a Marfan's syndrome (MFS) mouse model and has characteristics that are similar to those of fibrillin-1 dysfunction [23]. These findings have strongly suggested that microfibril formation through fibrillin-1 assembly plays an important role in PDL formation and function. However, the molecular mechanisms of fibrillin-1 microfibril assembly remain unclear as the microfibril-associated molecule that regulates or stabilizes fibrillin-1 microfibril formation has not yet been identified. Recent findings have revealed that ADAMSL6 β is essential for the development and regeneration of the PDL through the direct interaction of fibrillin-1 to promote microfibril assembly [23,24]. These findings have also suggested that the administration of fibrillin-1 microfibrils provides a novel therapeutic strategy for the treatment of periodontal disease.

We here review the present status of the periodontal tissue regeneration technologies that focus on the molecular mechanisms underlying development, regeneration and tissue engineering of periodontal tissue, and also discuss the potential of ECM administration therapy through the promotion of microfibril assembly as a novel therapeutic strategy for the essential functional recovery of periodontal tissue.

2. Development processes in periodontal tissue

The PDL has essential roles in tooth support, homeostasis and repair, and is involved in the regulation of periodontal cellular activities such as cell proliferation, apoptosis, the secretion of extracellular matrices, resorption and repair of the root cementum and remodeling of the alveolar bone [25,27]. To develop future methods to regenerate damaged PDLs, it will be important to understand the molecular basis of PDL development.

2.1 Molecular mechanisms underlying periodontal tissue development

The PDL is derived from the dental follicle (DF), which is located within the outer mesenchymal cells of the tooth germ and can generate a range of periodontal tissues including

the PDL, cementum and alveolar bone [21]. The DF is formed during the cap stage of tooth germ development by an ectomesenchymal progenitor cell population originating from the cranial neural crest cells [28]. Given the critical role that the progenitor cell population in the DF appears to play in the development of periodontal tissue, the developmental processes in this tissue are of considerable interest in terms of further understanding the biology of these cells (Figure 1). The differentiation of the DF proceeds as follows: i) during the tooth root-forming stage, the Hertwig's epithelial root sheath (HERS) comprising the inner- and outer-dental epithelia that initiate tooth root dentin formation is fragmented into the Malassez epithelium resting on the tooth root surface; ii) the DF migrates to the surface of the tooth root and differentiates into cementoblasts to form the cementum matrix [29,30]; iii) at almost the same time, the DF differentiates into the PDL on the cementoblasts in order to insert collagen fibers, known as Sharpey's fibers, into the cementum matrix. Fiber insertion also takes place along the alveolar bone and iv) both bone- and PDL-derived fibers finally coalesce in the PDL to form the intermediate plexus, which resembles tendinous tissue [31-33].

The DF has long been considered to be a source of multipotent stem cells (DFSCs), since these cells have the ability to migrate onto the tooth root surface to form periodontal tissue including cementum, PDL and alveolar bone during the tooth root-forming stage [32,34-37]. Previous studies have indicated that DF cells can form PDL-like tissues and cementum/bone-like structures after implantation into immunodeficient mice [38,39], supporting the notion that stem cells which can differentiate into PDL, cementoblast, osteoblast lineages are present in the DF [34,35]. To regenerate periodontal tissue, functional molecules which promote the differentiation of DFSCs into PDL need to be elucidated to enable a proper understanding of the mechanisms underlying periodontal tissue formation, including the pathways pertaining to PDL cell, cementum and alveolar bone differentiation.

2.2 Functional molecules involved in DF differentiation

Although the molecular mechanisms of DF development and differentiation remain to be determined, previous gene expression studies of mouse molar root development have suggested that some growth factors, including bone morphogenetic protein (BMP) 4, growth and differentiation factors (GDFs) 5, 6 and 7 [40-43], epidermal growth factors [44], *Shh* [45-47] and insulin-like growth factor (IGF)-1 [48], are involved in the growth or differentiation of the DF. Transcriptional factors such as *Scleraxis*, *Gli*, *Msx1*, *Msx2* and *Runx2* have also been shown to be involved in the differentiation of the DF into cementoblasts and in the mineralization of cementum [39,43,46,49]. Among these factors, GDFs and *scleraxis* are the most well characterized that are involved in tendon/ligament morphogenesis, suggesting that PDL development shares similar molecular mechanisms to those of tendon/ligament morphogenesis. With regard to

cementogenesis/osteogenesis of the DF, treatment of this tissue with BMP-2 and BMP-7 has been found to induce mineralization ability. In addition, previous findings suggest that PDL cells harbor mineralization inhibitory mechanisms that enable them to maintain a ligament structure across the mineralized tissue, including the alveolar bone and cementum, during PDL development [50-52]. These observations strongly suggest that the tendon/ligament-related cytokines, the BMPs, and inhibitors of mineralization are linked to the restoration of the tendinous structure of the PDL. The mechanisms involving these factors may also have a role in preventing ankylosis of the PDL.

3. Regeneration therapies for PDL defects

A partial restoration of periodontal tissue has been achieved previously using a guided tissue regeneration (GTR) technique which provides an adequate space and favorable niche for the repair of periodontal defects using barrier membrane [53]. From the results of these GTR therapies, regeneration of the PDL has been shown to be critical for recovering the connection between the cementum on the root surface and the alveolar bone.

To regenerate periodontal tissue that has been destroyed by periodontal disease requires the recruitment of PDL stem cells (PDLSCs) to properly reconstitute the PDL structure including its extracellular components such as the collagen and elastic fibril systems [32,33]. Recent studies of stem/progenitor cells have provided considerable new insights that have furthered our understanding of PDLSCs, which can differentiate into periodontal tissue cell lineages such as PDL, cementum and alveolar bone [14,54]. PDLSCs will have utility for the future development of stem cell transplantation therapies and tissue engineering applications to restore periodontal organ function as they replace damaged areas with enriched and purified stem cells and thereby achieve PDL repair (Figure 2) [14]. The biological potential of PDLSCs to stimulate the regeneration of periodontal tissue can now be realized by the local application of human recombinant cytokines.

3.1 Stem cell therapies

PDLSCs have been isolated from human PDL tissue by single-colony selection and magnetic activated cell sorting. PDLSCs express the mesenchymal stem cell markers STRO-1 and CD146/MUC18, and can differentiate into cementoblast-like cells, adipocytes and fibroblasts [14]. In addition, PDLSCs show the capacity to generate a cementum/PDL-like structure and contribute to periodontal tissue repair on transplantation into immunocompromised rodents. Clonal PDLSC analysis has further revealed that these cells show a similar phenotype to DFSCs since they also express *RUNX-2*, *Col I*, *ALP*, *OPN*, *OCN*, *RANKL*, *OPG*, *scleraxis*, *periostin*, *Col XII* and *alpha-SMA* mRNAs [54]. Importantly, PDL tissue collected from one tooth can give rise to many stem cells because of their high proliferation capacity *ex vivo*. Recently also, it has been shown that the transplantation of autologous PDLSCs obtained from the